Stepwise Hydration of Protonated Carbonic Acid: A Theoretical Study

M. Prakash,[†] V. Subramanian,*[,†] and Shridhar R. Gadre*[,‡]

Chemical Laboratory, Central Leather Research Institute, Central Leather Research Institute, Adyar, Chennai 600 020, India, and Department of Chemistry, University of Pune, Pune 411 007, India

Received: December 10, 2008; Revised Manuscript Received: September 10, 2009

The gas-phase geometries, binding energies (BEs), and sequential binding energies (SBEs) of protonated carbonic acid (PCA)−water (W) clusters ($PCAW_n$, where $n = 1-6$) have been calculated using density functional theory (DFT) with Becke's three-parameter hybrid exchange functional and the Lee−Yang−Parr correlation functional (B3LYP) and M05-2X methods. The presence of wirelike structures of protonated water in $PCAW_n^x$ clusters is evident from the results. The results indicate that a proton is transferred from PCA to its immediate water molecule in the linear and monohydroxy clusters of PCA. The involvement of the Eigen cation and Grotthuss type of mechanism in the proton transport is observed from the sequential hydration energies and from the calculated vibrational spectra. Although geometrical parameters clearly reveal the presence of the Eigen core, calculated lower-energy vibrational modes provide clues about the involvement of the sequence Eigen → Zundel → Eigen in the proton transfer.

1. Introduction

Because hydrolysis of CO_2 is an important process in natural science, several experimental and theoretical studies have been carried out on carbonic acid (H_2CO_3).[1−11] These studies have revealed that both carbonic acid (CA) and the weakly bound isomer of a $H_2O\cdots CO_2$ complex are short-lived intermediates in the hydrolysis of CO_2. The formation of H_2CO_3 from CO_2 and H_2O has been investigated using a variety of quantum chemical methods.[12] In the same study, the role of microsolvation of CO_2 in the formation of CA was also addressed.[12] High-resolution spectroscopic techniques have provided indirect evidence for the existence of CA in the gas phase.[13] On the other hand, theoretical studies have shown that isolated H_2CO_3 should be stable, although it decomposes into H_2O and CO_2 in the presence of water.[14] Recently, Andrei et al. detected the protonated carbonic acid $C(OH)_3^+$ in the gas phase for the first time using high-resolution infrared (IR) spectroscopy.[15] They also used density functional theory (DFT) with Becke's three-parameter hybrid exchange functional and the Lee−Yang−Parr correlation functional (B3LYP) to predict the structure and stability of different isomers of PCA.[15]

Previous quantum chemical calculations on PCA have predicted the existence of different isomers on the $[CH_3O_3]^+$ potential-energy surface.[16] The linear hydrogen-bonded (H-bonded) $H_3O^+\cdots CO_2$ complex (A) is the most stable isomer.[17] The protonation of CA at the carbonyl group leads to two planar isomers: the *anti*-trihydroxycarbenium ion (C_{3h}) and the *syn*-trihydroxycarbenium ion (C_s symmetry). In this work, these two complexes are referred to as B and C, respectively. The fourth isomer of $[CH_3O_3]^+$ arises as a result of the protonation of H_2CO_3 at a hydroxyl group. It is a nonplanar molecule with C_1 symmetry. This hitherto undetected complex is designated as D. Previous DFT calculations on these molecules have shown the stabilities of these isomers to be in the order A > B > C > D.[16]

Egsgaard et al. reported that PCA is generated by the consecutive elimination of a vinyl radical and an alkene from the radical cation of dialkylcarbonates.[16a] They found that protonated carbonic acid forms symmetrical trihydroxy species and that fragmentation of unsymmetrical isomer leads to protonated carbon dioxide and water. Olah and White illustrated that PCA is remarkably stable in superacidic media and might play an important role in the biological carboxylation process, which involves a proton-transfer mechanism.[18a] Nuclear magnetic resonance (NMR), IR, Raman, and X-ray crystallography studies of $C(OH)_3^+$ in superacid solutions or corresponding salts confirm the existence of isomer B.[18] Recently, the structure of PCA in the gas phase was studied using mid-IR spectroscopy.[19] Combined evidence gathered by these studies points out that isomer B is stable in both the solution and gas phases.[18,19]

With a view toward understanding proton transfer in various model systems, numerous experimental and theoretical studies have been carried out.[20] The role of the proton in $H^+(H_2O)_n$ clusters ($n = 1-27$) has been investigated using high-resolution IR spectroscopy techniques and various levels of electronic structure calculations.[21] The presence of Eigen[22] (H_3O^+) and Zundel[23] ($H_2O\cdots H^+\cdots H_2O$) cations in protonated water clusters was observed in earlier investigations. It has been found that small protonated water clusters ($n \sim 10$) form chain structures and that nanometer-scale cages form for $n > 21$.[21a] The dynamics of proton transport in water has received widespread attention.[24] It is possible to note that the position of the excess proton in these clusters varies sensitively with the number of water molecules and the geometry of the clusters.[25−27] Voth and coworkers used multistate empirical valence bond theory and ab initio molecular dynamics simulations to study hydrated protons in methanol−water solutions.[28−31] These investigations provided the modern version of Grotthuss-like mechanism that is typically described as proton transfer from H_3O^+ to H_2O.[25,32]

The transfer of H^+ along a H-bonded water chain, or proton wire, is thought to be an important mechanism in various

* To whom correspondence should be addressed. E-mail: subuchem@hotmail.com (V.S.), subbu@clri.res.in (V.S.), gadre@chem.unipune.ernet.in (S.R.G.). Tel.: +91 44 24411630 (V.S.), +91-20-2560-1398 (S.R.G.). Fax: +91 44 24911589 (V.S.), +91-20-2569-1728 (S.R.G.).

[†] Central Leather Research Institute.

[‡] University of Pune.

10.1021/jp904576u CCC: $40.75
Published on Web 10/07/2009

chemical and biological processes.[33] The structure of a proton wire inside a carbon nanotube was investigated to understand the mechanism of proton conduction in biological systems and the effect of structural confinement on the proton-transport process.[34] Water wires are responsible for the selective proton conductivity in pure lipid bilayers,[32] the ATP synthase complex,[35] bacteriorhodopsin,[36] and pendadecapeptide gramicidin A.[37] In human carbonic anhydrase II, a chain of three water molecules plays a crucial role in the proton transfer.[38] The application of proton wires in molecular switches has also been reported.[39] The proton-transfer mechanism between aqueous Brønsted acids and bases has been studied in real time using ultrafast IR spectroscopy.[40] This study demonstrated the Grotthuss-type sequential proton-hopping mechanism through water bridges in acid−base reactions.

Although numerous studies have been carried out on proton wires, we felt that addressing the question of how a protonated molecule interacts with water molecules and conducts proton would enhance our understanding of proton transfer in other systems. Hence, we undertook a systematic study on the sequential hydration of isomers A−C of PCA. In this context, selection of the appropriate quantum chemical computational method to probe the structure and stability of these hydrated clusters is necessary.

An analysis of various quantum chemical methods for probing molecular hydration has been made.[27,41] In a recent work, hydration of different mono- and divalent metal ions was studied using DFT(B3LYP); Møller−Plesset second-order perturbation (MP2) and coupled-cluster theory with single, double, and triple excitations [CCSD(T)]; and the G3 quantum chemical method.[42a] Double- and triple-ζ basis sets containing both polarization and diffuse functions were employed in this study. Total and sequential binding energies for hydration of metal ions were calculated for metal−water clusters containing one to six water molecules. In the same study, a systematic benchmarking of the performance of the above-mentioned methods was reported.[42a] Although no single method was found to consistently show excellent performance for the hydration of all metal ions, the B3LYP/6-311++G** method seemed to be the most economical computational method. It was also noted that this method provides correct trends in sequential hydration of energies of different metal ions containing more than four water molecules. Earlier studies on stepwise hydration by the research groups of the authors of the present work, carried out at the HF or DFT level of theory,[42b−d] included substrates such as crown ether, cytosine dimer, and uracil. Recently, several new density functionals have been developed for addressing a variety of issues in chemical and biological systems.[43] For example, Truhlar and co-workers found that the new hybrid meta exchange-correlation functional M05-2X is quite suitable for probing H-bonding and noncovalent interactions as compared to the other functionals.[44] Hence, the present study employs Hartree−Fock (HF), DFT(B3LYP), and DFT(M05-2X) methods for probing the structures and stabilities of hydrated clusters of isomers A−C of PCA.

2. Computational Details

The molecular structures and hydration patterns of isomers A−C are presented in Scheme 1. Various initial and corresponding optimized geometries considered in this study are provided in the Supporting Information (Figure S1). The water clusters of isomers A, B, and C are designated, respectively, as AW_n, BW_n, and CW_n (where $n = 1-6$).

As seen in Scheme 1, three different patterns of hydration of isomer A are considered, corresponding to (i) linear (l), (ii) branched (b), and (iii) cyclic (c) hydration of the H_3O^+ fragment in PCA. These clusters are referred to as AW_n^l, AW_n^b, and AW_n^c ($n = 1-6$), respectively. It can be seen from Figure S1 (Supporting Information) that clusters with CO_2-W interactions were first thought to be important. However, these initial geometries were found to undergo reorganization during geometry optimization. Further, it may be noted that, after optimization, water molecules tend to interact with the H_3O^+ moiety rather than with CO_2. Hence, in this study, the AW_n^l, AW_n^b, and AW_n^c ($n = 1-6$) types of clusters were considered only for completeness.

Three different patterns of hydration in isomers B and C considered in this study are (i) interaction of water molecules with any one of the hydroxyl groups, referred to as monohydroxy hydration (BW_n^m, and CW_n^m); (ii) interaction of water molecules with any two hydroxyl groups, designated as dihydroxy hydration (BW_n^d and CW_n^d); and (iii) interaction of water molecules with all of the hydroxyl groups, referred to as trihydroxy hydration (BW_n^t and CW_n^t).

The geometries of all clusters were optimized using the HF, DFT(B3LYP), and DFT(M05-2X) methods with the 6-31+G* and 6-311++G** basis sets. All calculations were performed using the Gaussian 98W[45] and Gaussian 03 (revision E.01) suites of programs.[46] Because the reliability of the B3LYP/6-31+G* level of calculation in predicting the vibrational frequencies of protonated clusters was confirmed in previous studies,[47,48] the same method was used here. Vibrational frequencies were scaled by a factor of 0.973.[47] The geometries of all clusters were minima on their respective potential energy surfaces at the B3LYP/6-31+G* level of theory. The binding energies (BEs) of all clusters were calculated using the supermolecule approach and corrected for basis set superposition error (BSSE) using the counterpoise (CP) procedure suggested by Boys and Bernardi[49]

$$\mathrm{BE} = -(E_{\mathrm{cluster}} - \sum_{i=1}^{n} E_i) \qquad (1)$$

where E_{cluster} is the total energy of the cluster, E_i is energy of the monomer, and n is the total number of monomers in the cluster. Specifically, BSSE was estimated for each monomer by computing the energy corresponding to the geometry in the cluster with the n-mer basis set. The BSSE-corrected sequential binding energies (SBEs) of various clusters were calculated as per eq 1 using the procedure explained in an earlier report[42]

$$E_{\mathrm{SBE}} = -\{E_{(\mathrm{PCAW}_n)} - [E_{(\mathrm{PCAW}_{n-1})} + E_{(\mathrm{H_2O})}]\} \qquad (2)$$

Here, E_{SBE} is the sequential binding energy and $E_{(\mathrm{PCAW}_n)}$, $E_{(\mathrm{PCAW}_{n-1})}$, and $E_{(\mathrm{H_2O})}$ are the total energies of clusters with n water molecules, $n - 1$ water molecules, and one water molecule, respectively, obtained at the B3LYP/6-311++G** level.

3. Results and Discussion

3.1. Hydration of Isomer A. ***3.1.1. Linear-Type Clusters (AW_n^l).*** Scheme 1 shows that the most stable structure of isomer A exists as $CO_2\cdots H_3O^+$. In this isomer, water molecules strongly interact with the H_3O^+ moiety of PCA and form structures that are similar to those of protonated water clusters.[21] Figure 1 illustrates the optimized geometries of AW_n^l ($n = 1-6$), along with the atom numbering and bond distances obtained

SCHEME 1: Hydration Patterns of Protonated Carbonic Acid (PCA): Isomers A, B, and C

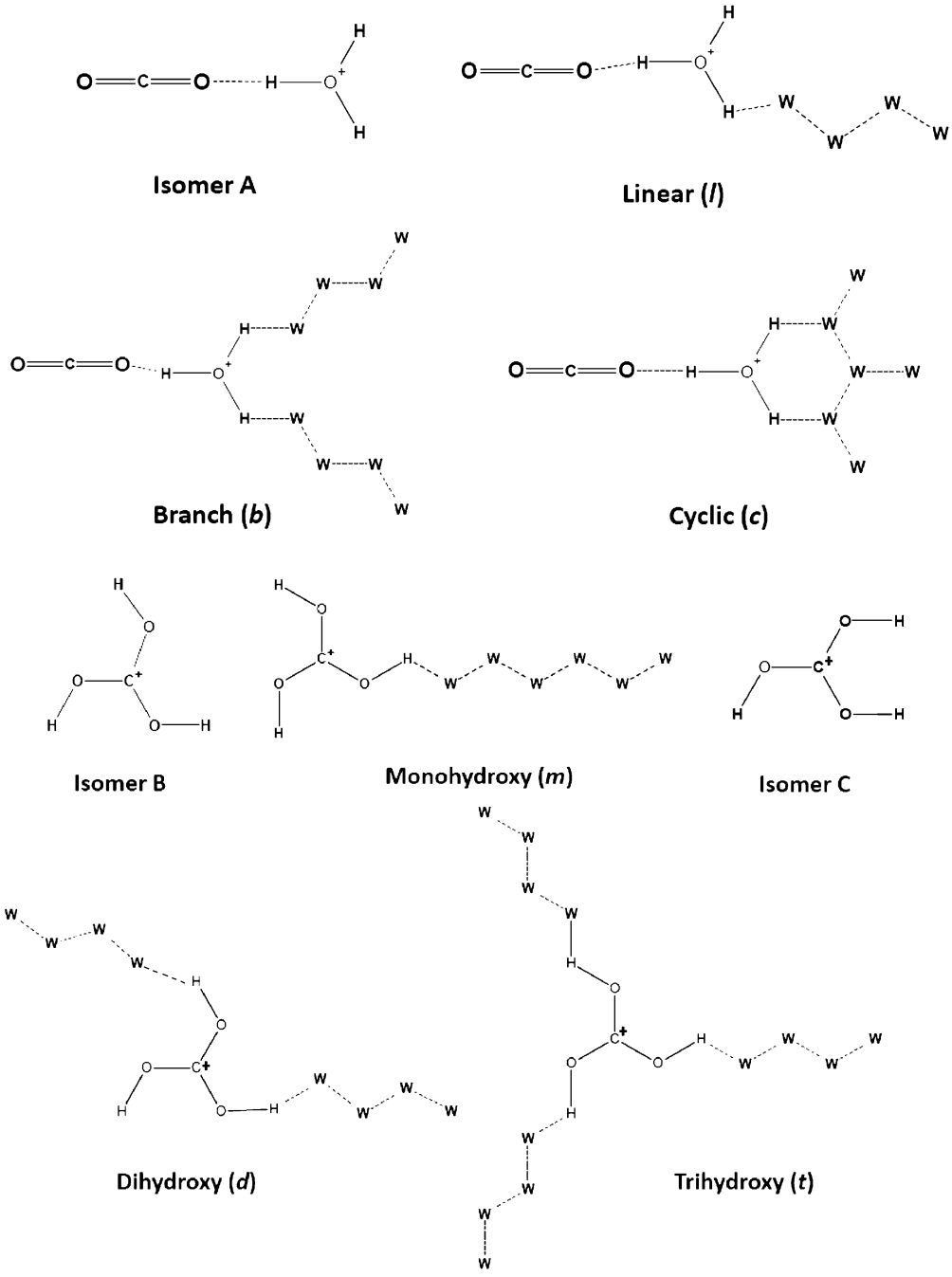

from HF (normal), B3LYP (bold), and M05-2X (bold and italic) calculation using the 6-311++G** basis set. Although calculations were carried out using three different levels of theory, the geometrical parameters obtained from DFT (M05-2X)/6-311++G** are considered for analysis. In isomer A, the O1−C1 and C1−O2 bond lengths are 1.135 and 1.172 Å, respectively. The O2···O3 H-bond distance is 2.531 Å. The distance between O2 and H1 is 1.513 Å. The O−H bond lengths of the H_3O^+ fragment, which are not involved in the H-bonding, are equal to 0.972 Å.

In cluster AW_1^l, the water molecule forms a H-bond with the H_3O^+ fragment. This cluster consists of two H-bonds: O2···O3 (2.714 Å) and O3···O4 (2.413 Å). It can be observed from these H-bonding distances that, compared to the O2···O3 distance in isomer A, the one in AW_1^l is 0.2 Å larger. This indicates that the H_3O^+ is closer (H-bonded) to the water molecule than the CO_2 fragment. Further, increases in the O2···H1 and O3···H3 distances and a decrease in the O3−H1 distance can also be observed when compared to the values for isomer A. The shifting of the proton from isomer A to water is evident from the changes in the geometrical parameters.

Similar variations in the geometrical parameters of AW_2^l can be found from Figure 1. This cluster has three H-bonds, viz., O2···O3, O3···O4, and O4···O5. The corresponding distances are 2.847, 2.424, and 2.488 Å. These values clearly reveal that the proton shifts from the H_3O^+ moiety to the neighboring water molecules. Because of proton transport from isomer A to water, the geometrical parameters of the other parts of the cluster undergo considerable change. As water molecules are sequentially added to AW_2^l in a linear fashion, proton transport takes place from one water molecule to its immediate neighbor in a manner akin to the Grotthuss mechanism. A similar pattern in

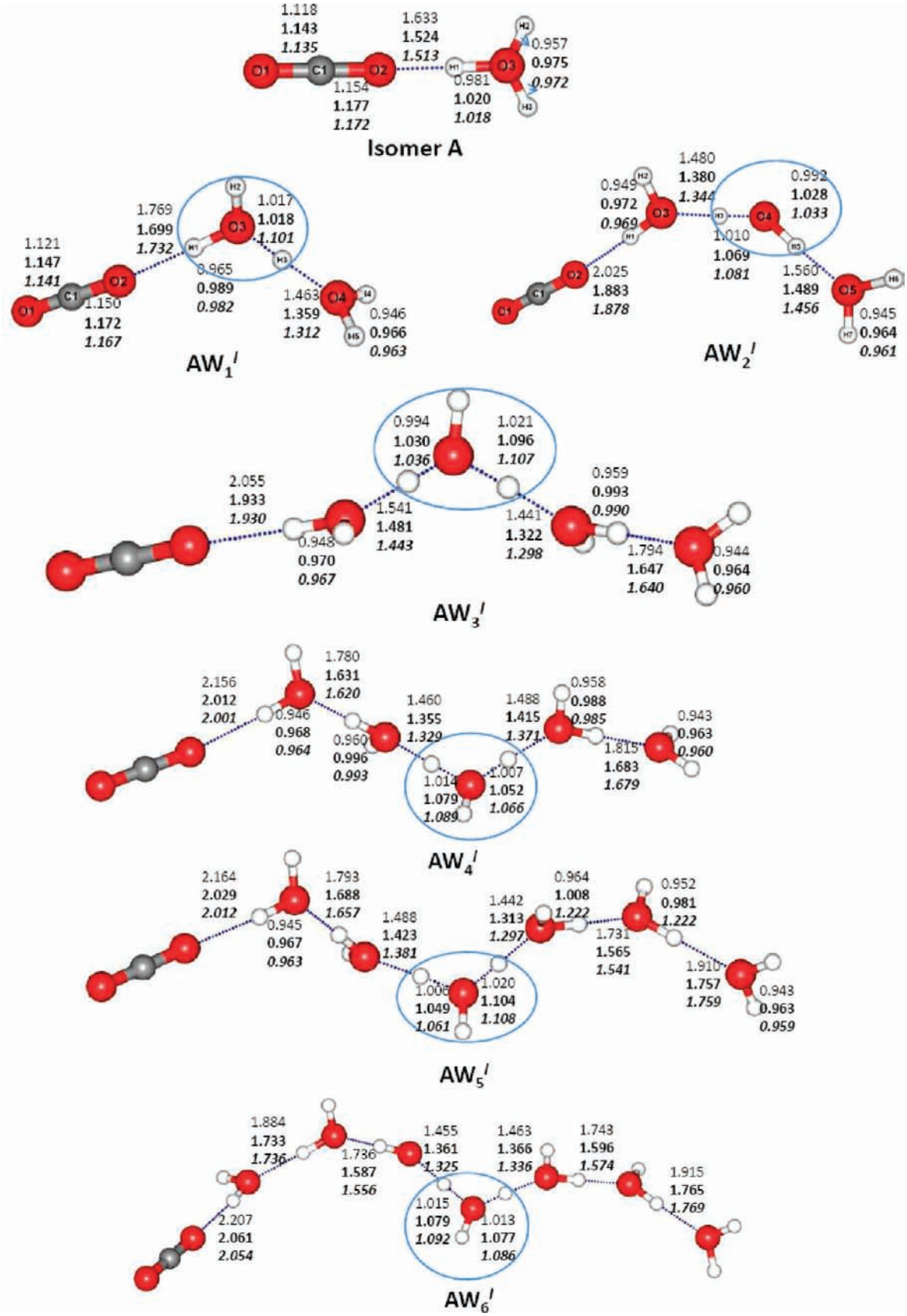

Figure 1. Optimized geometries of AW_n^l linear clusters (where $n = 1-6$) at the HF/6-311++G** (normal), B3LYP/6-311++G** (bold), and M05-2X/6-311++G** (bold and italic) levels of theory. The blue circles indicate the presence of the Eigen core cation. Distances are in angstroms.

proton transport has been observed in the other clusters. Figure 1 shows that the H-bond distances in the middle region of the water wire are shorter than those in the peripheral regions.

3.1.2. Branched-Type Clusters (AW_n^b). The optimized geometries of AW_n^b clusters (where $n = 2-6$) are depicted in Figure 2. The geometrical parameters indicate that there is no

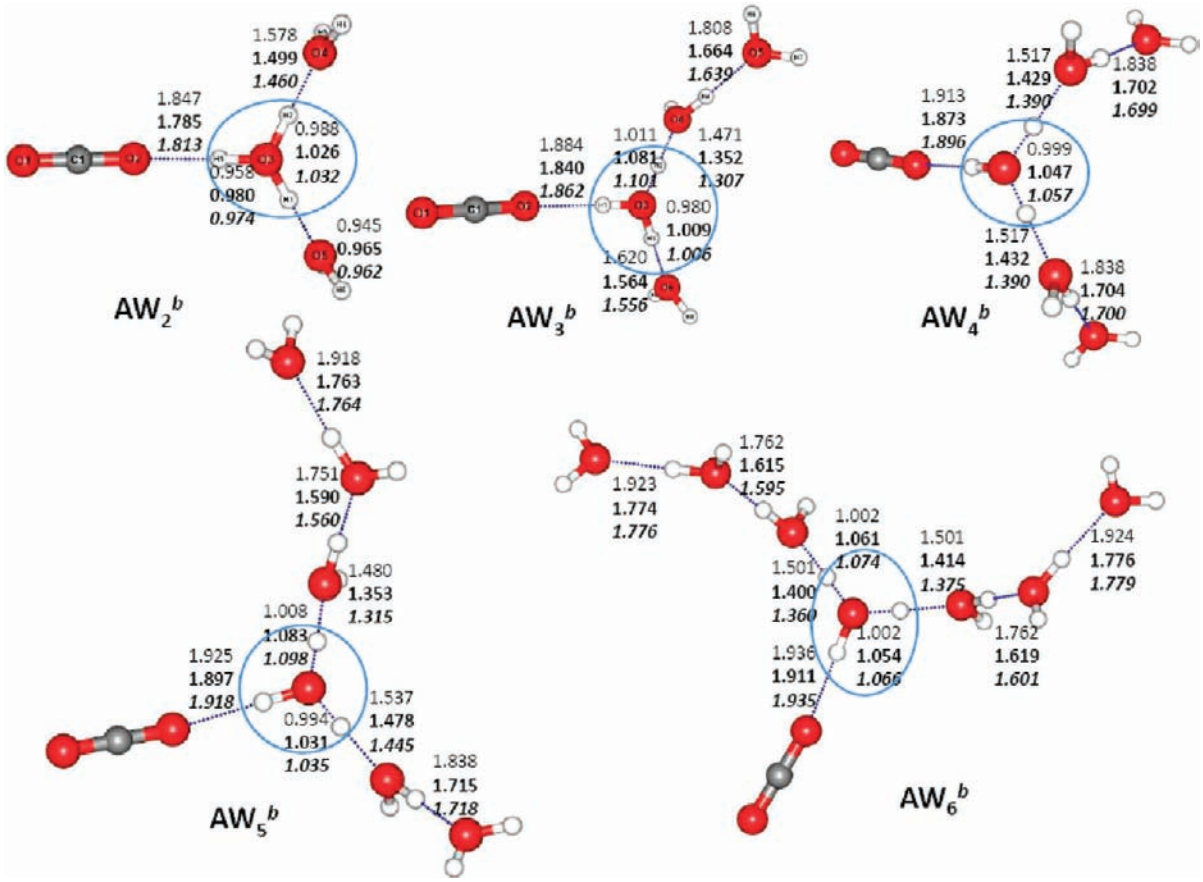

Figure 2. Optimized geometries of AW_n^b branched clusters (where $n = 2-6$) at the HF/6-311++G** (normal), B3LYP/6-311++G** (bold), and M05-2X/6-311++G** (bold and italic) levels of theory. The blue circles indicate the presence of the Eigen core cation. Distances are in angstroms.

proton movement in these clusters. Further, in AW_2^b, the proton is bound to the CO_2 fragment and two water molecules in the first solvation shell. It was found from the calculations that further addition of water molecules does not favor proton transport in any preferential direction.

3.1.3. Cyclic Clusters (AW_n^c). Earlier studies on protonated water clusters have provided information about the existence of cyclic clusters.[48a] Similar structures are also observed in isomer A. The optimized geometries of cyclic clusters AW_n^c ($n = 3-6$) are presented in Figure 3. The tetrameric core structure stabilizes the AW_n^c clusters ($n = 3-6$), except in the case of AW_5^{c1} (cyclic hexamer). The geometrical parameters confirm the involvement of the Eigen cation in proton transfer in all of the A-type clusters.

3.2. Hydration of Isomer B. ***3.2.1. Monohydroxy Hydrated Clusters (m).*** Figure 4 displays the optimized geometries of isomer B and BW_n^m clusters ($n = 1-6$). The results indicate that the three O−H (0.974 Å) and C−O (1.275 Å) bond lengths and the three C−O−H angles are equal in isomer B. The calculated O−H distance from IR spectroscopy is 0.976 Å.[15] The C−O bond distance in the salt of PCA is 1.231 Å.[19] The results reveal that monohydroxy hydrated clusters of isomer B form linear chainlike structures that are akin to those of AW_n^l. Thus, proton-transfer patterns in these clusters are similar to those of AW_n^l. In BW_1^m, the O1···O4 H-bond distance is 2.430 Å. There is a slight decrease in the length of the C1−O1 bond due to H-bonding. As a result, there is a significant increase in the O1−H1 bond length from 0.974 to 1.093 Å. There are no appreciable changes in the free O−H bond lengths upon formation of a cluster.

In BW_2^m, the cluster has two H-bonds: O1···O4 (2.457 Å) and O4···O5 (2.511 Å). It is interesting to note that the O1−H1 distance increases by 0.283 Å due to the addition of one water molecule to BW_1^m and simultaneously the H1−O4 distance decreases by 0.255 Å. This evidence shows that the proton moves slightly away from the CA moiety to the water chain. As the chain length grows from two to six water molecules, the proton shifts from one water molecule to its neighbor in the chain. It can be observed from the geometrical parameters that the distances are shorter for the inner H-bonds than for those present in the periphery. In all of the clusters, most of the H-bond angles are nearly equal to 175°. The presence of the Eigen core in the proton transfer can be seen from the geometrical parameters of all of the clusters.

3.2.2. Dihydroxy Hydrated Clusters (d). The dihydroxy hydrated clusters of isomer B are depicted in Figure 5. The presence of the Eigen core is clearly evident from the geometrical parameters displayed therein. In BW_2^d, two water molecules are H-bonded to two C−O groups, such as C1−O1 and C1−O2. There are noticeable changes in the H-bond parameters of BW_2^d when compared to those of BW_1^m. The O1···O4 and O2···O5 H-bond distances in BW_2^d are 2.472 and 2.482 Å, respectively, which are higher than that in BW_1^m. The geometrical parameters indicate that the proton is equally shared between the two water molecules. A similar trend is seen in other clusters with equal numbers of water molecules on both sides of isomer B. Proton transfer is not observed in these cases.

With a view towards probing proton transport, unequally hydrated clusters of B were considered. These clusters are designated as $BW_n^{d(i+j)}$ ($n = 2-6$, $i + j = n$). In these clusters, one of the O−H groups is H-bonded to i water molecules and the other O−H group is H-bonded to j water molecules. The calculated geometrical parameters provide evidence for proton transfer in clusters BW_4^{d1}, BW_5^{d1}, BW_5^{d2}, BW_6^{d1}, BW_6^{d2}, BW_6^{d3},

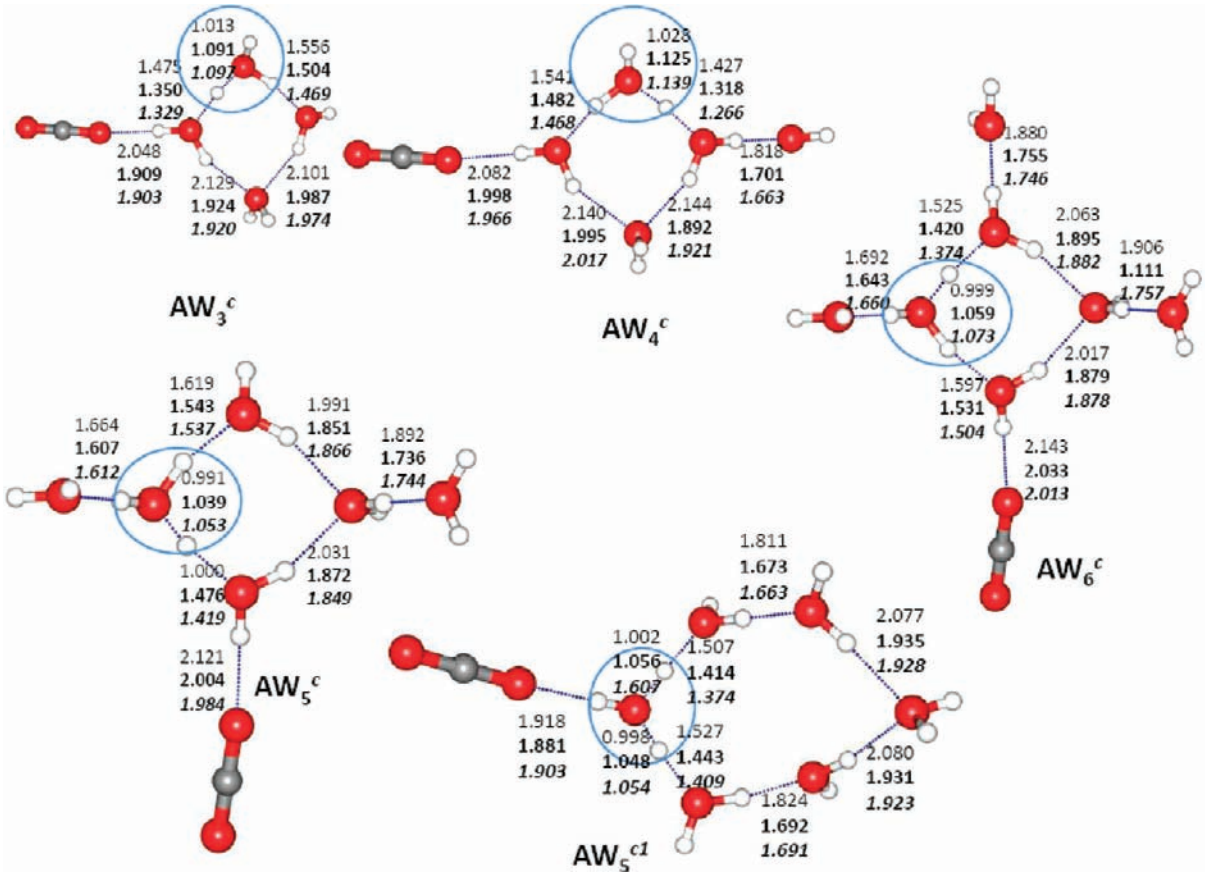

Figure 3. Optimized geometries of AW_n^c cyclic clusters (where $n = 3-6$) at the HF/6-311++G** (normal), B3LYP/6-311++G** (bold), and M05-2X/6-311++G** (bold and italic) levels of theory. The blue circles indicate the presence of the Eigen core cation. Distances are in angstroms.

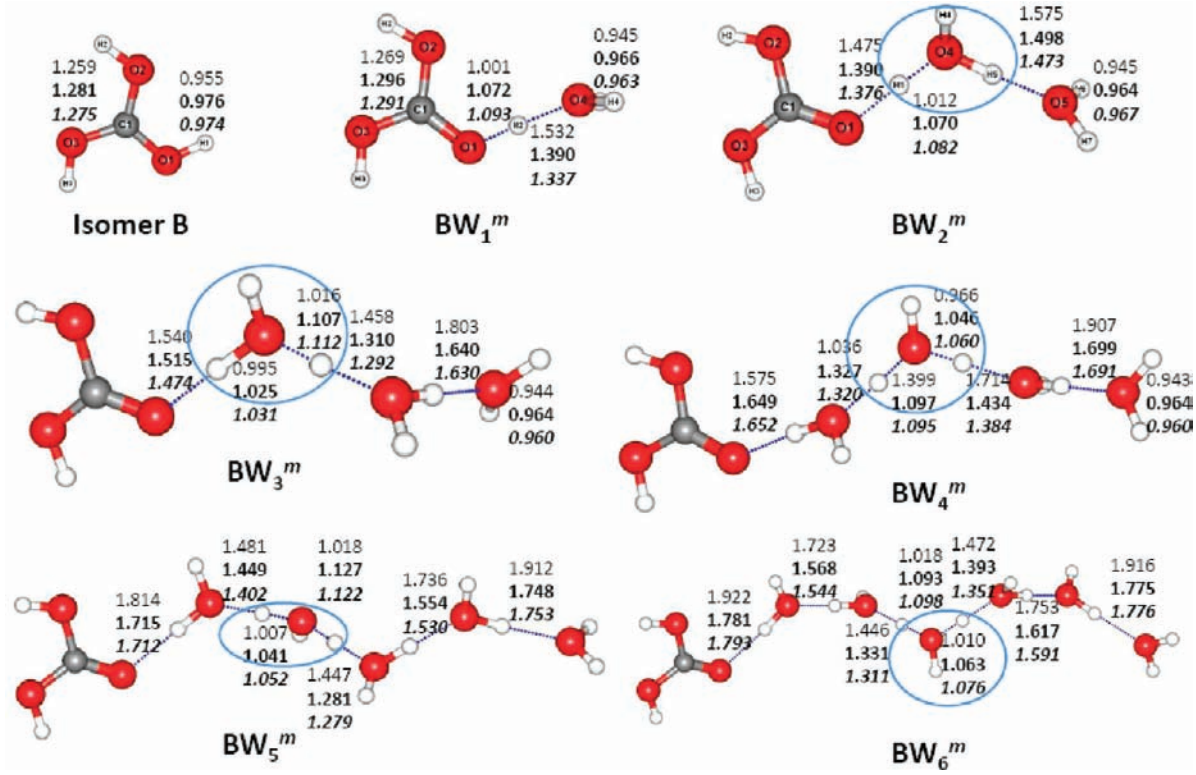

Figure 4. Optimized geometries of BW_n^m monohydroxy clusters (where $n = 1-6$) at the HF/6-311++G** (normal), B3LYP/6-311++G** (bold), and M05-2X/6-311++G** (bold and italic) levels of theory. The blue circles indicate the presence of the Eigen core cation. Distances are in angstroms.

and BW_6^{d4}. The unequal environment leads to changes in the charge delocalization arising from the loss of symmetry and resonance in isomer B. As a result, proton transfer takes place form isomer B to water in the BW_n^{di+j}, where i≠j type

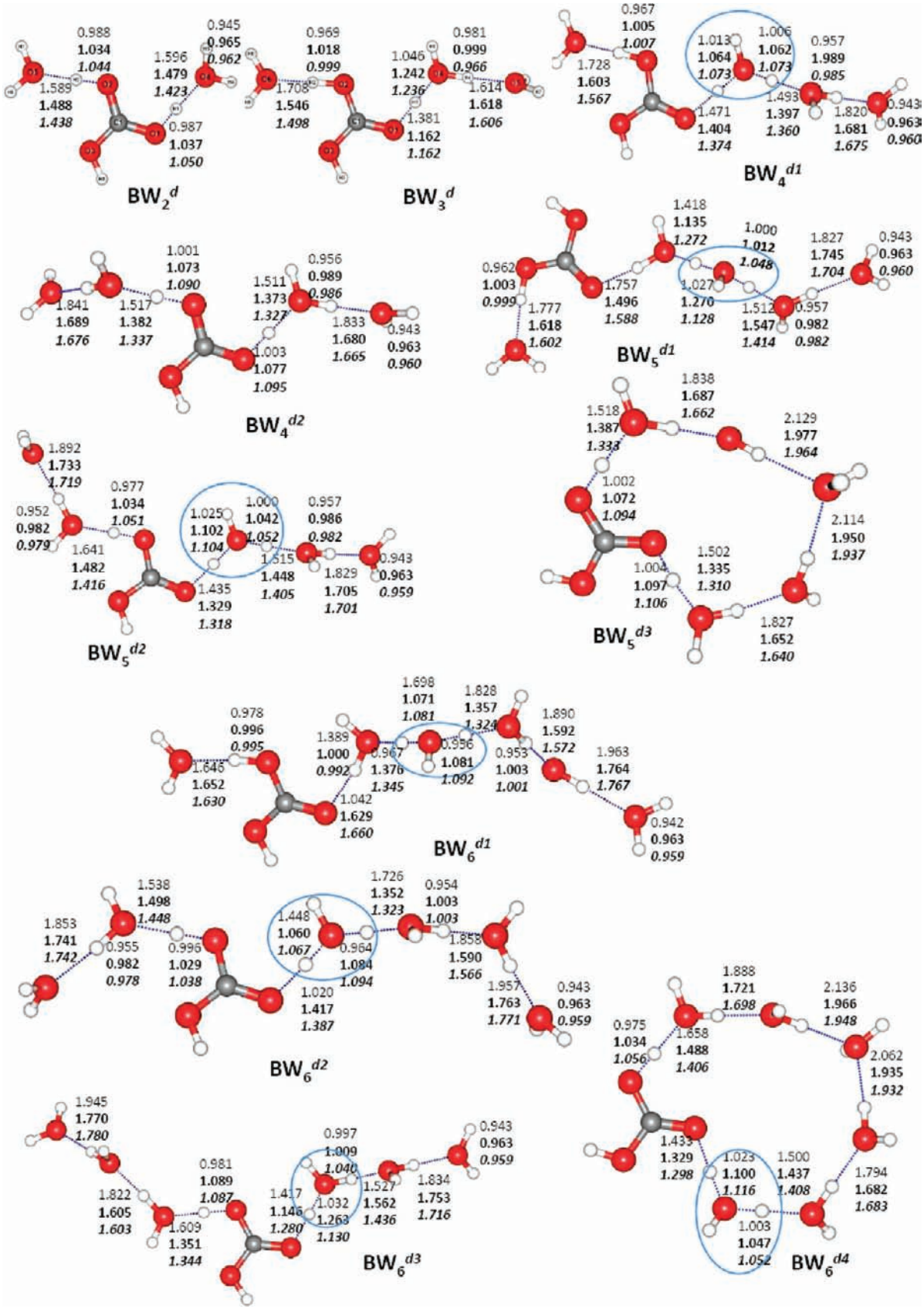

Figure 5. Optimized geometries of BW_n^d dihydroxy clusters (where $n = 2-6$) at the HF/6-311++G** (normal), B3LYP/6-311++G** (bold), and M05-2X/6-311++G** (bold and italic) levels of theory. The blue circles indicate the presence of the Eigen core cation. Distances are in angstroms.

of clusters. It is observed from Figure 5 that $n = 5$ and 6 clusters form cyclic structures in addition to the linear structures.

3.3. Hydration of Isomer C. ***3.3.1. Monohydroxy Hydrated Clusters (m).*** The optimized geometries of isomer C and its water clusters (CW_n^m, $n = 1-6$) are presented in Figure 6. The

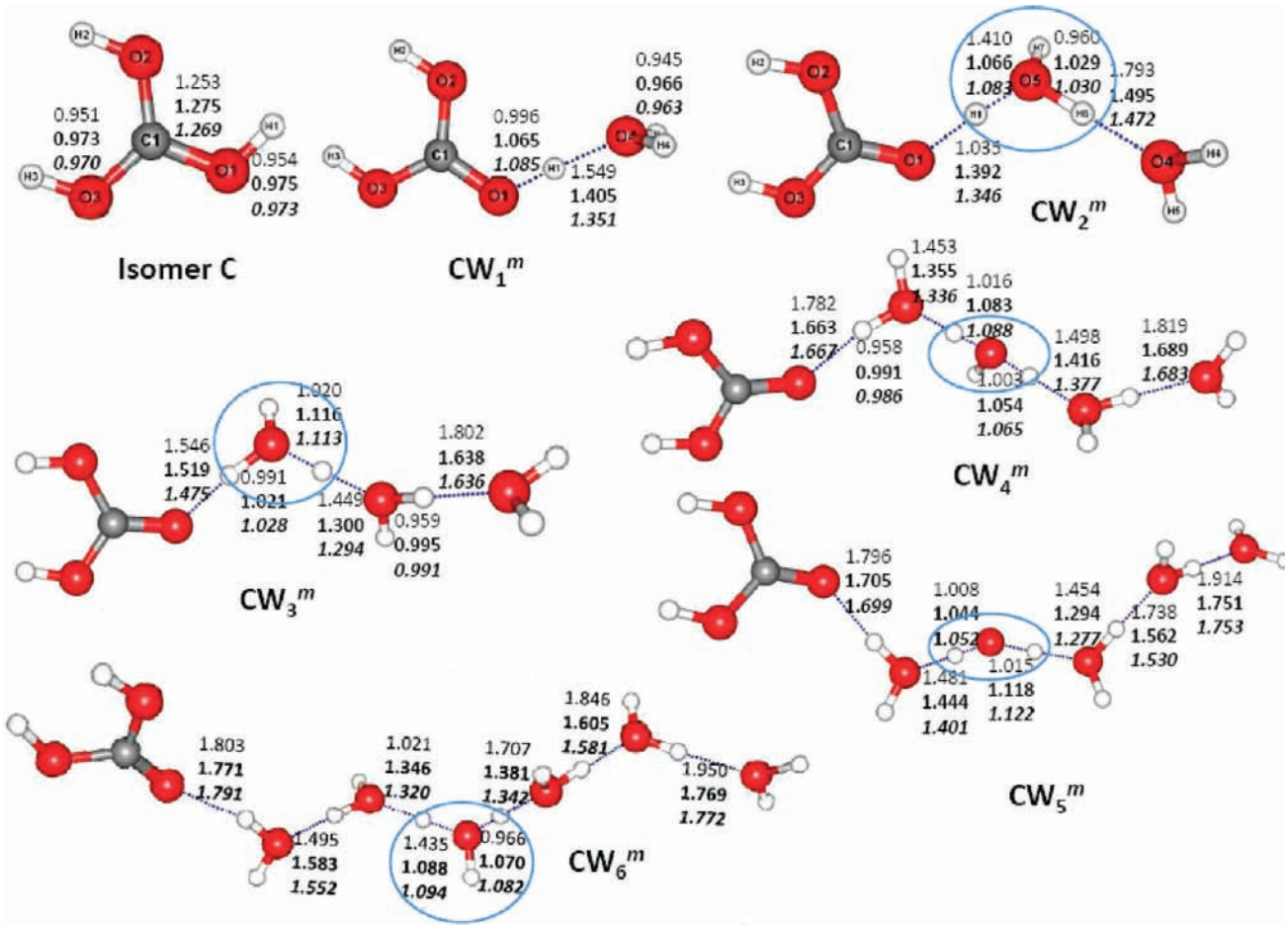

Figure 6. Optimized geometries of CW_n^m monohydroxy clusters (where $n = 1-6$) at the HF/6-311++G** (normal), B3LYP/6-311++G** (bold), and M05-2X/6-311++G** (bold and italic) levels of theory. The blue circles indicate the presence of the Eigen core cation. Distances are in angstroms.

O1−H1 distance of CW_1^m is longer than that in isomer C, which indicates the movement of proton from isomer C to the water molecule. The movement of the excess proton from isomer C to the neighboring water is evident from the geometrical parameters of CW_2^m. The subsequent addition of water molecules to CW_1^m clusters in a linear fashion enables the transfer of the excess proton from one water molecule to other. The proton transfer in water clusters of isomer C is comparable to that in the linear and monohydroxy hydrated clusters of isomers A and B, respectively.

3.3.2. Dihydroxy Hydrated Clusters (d). Figure 7 illustrates the geometries of dihydroxy hydrated clusters of isomer C. The existence of cyclic clusters of isomer C (except CW_2^d) can be seen from Figure 7. In cluster CW_1^d, the lone pairs on the oxygen atom interact with isomer C to form a bifurcated H-bond. In CW_2^d, two water molecules separately bind with the two hydroxyl groups of isomer C. Cyclic motifs such as those found in $(H_2O)_4$ and $(H_2O)_5$ are observed in clusters CW_3^d, CW_4^d, CW_5^d, and CW_6^d. There is no significant movement of the excess proton beyond the first hydration shell (i.e., hydration of hydroxyl groups).

3.3.3. Trihydroxy Hydrated Clusters (t) of Isomers B and C. Optimized geometries of trihydroxy hydrated clusters of isomers B and C are shown in Figure 8. Only the symmetrically hydrated BW_n^t and CW_n^t clusters ($n = 3$ and 6) are included in this category. The geometrical arrangements of BW_3^t and CW_3^t are similar to that of the symmetrically hydrated Eigen cation. CW_6^t forms a cyclic structure owing to the orientation of the O−H groups in isomer C. It was found from the results that higher-order water clusters of isomers B and C favor the formation of cyclic structures. The calculated geometrical parameters show that there is no significant proton movement from the PCA moiety to the water molecules in these clusters.

3.4. Comparison of Geometrical Parameters. In this study, the geometries of various clusters were obtained by three different methods employing three different basis sets. As expected, the geometrical parameters are sensitive to the level of the calculations and the quality of the basis sets. The O2···O3 distance in isomer A at the HF level using the 6-31G*, 6-31+G*, and 6-311++G** basis sets was calculated as 2.657, 2.664, and 2.614 Å, respectively. The same distance at the B3LYP level with the above-mentioned basis sets was 2.569, 2.592, and 2.544 Å, respectively. For the same basis sets, the M05-2X method predicts the distance to be 2.579, 2.602, and 2.531 Å, respectively. The calculated O···O distance using the three different basis sets varies as 6-31+G* > 6-31G* > 6-311++G** at all calculation levels. The results obtained at different levels of calculation using the 6-311++G** basis set were considered for further analysis. It can be observed from Figure 4 that the O−H distance in isomer B is slightly shorter at the M05-2X level than at the B3LYP level, which is longer than the corresponding value at the HF level. The geometrical parameters of CW_n clusters are similar to those in clusters with isomer B.

Because the sequential addition of water molecules shifts the proton from one molecule to its neighbor, the effect of calculation level was analyzed for O−H···O distances in various $PCAW_n^x$ clusters. Comparison of the geometrical

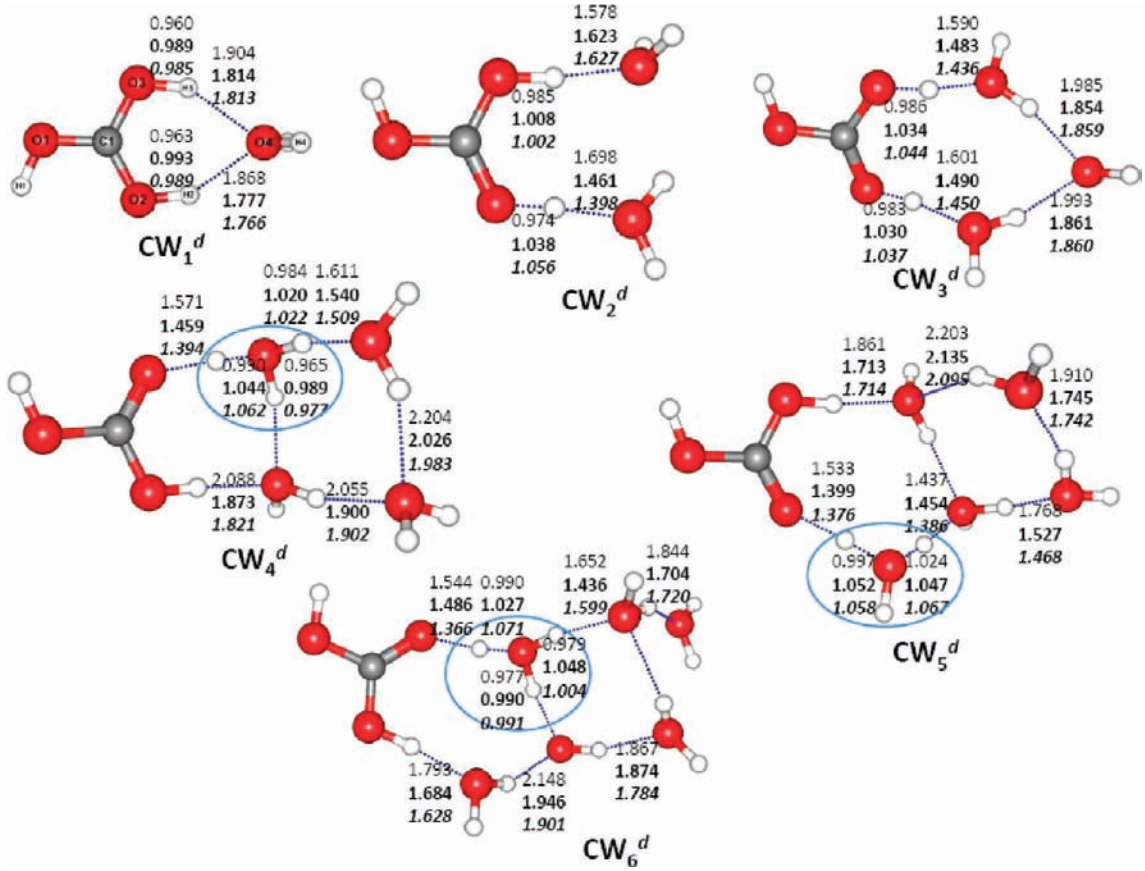

Figure 7. Optimized geometries of CW_n^d dihydroxy clusters (where $n = 1-6$) at the HF/6-311++G** (normal), B3LYP/6-311++G** (bold), and M05-2X/6-311++G** (bold and italic) levels of theory. The blue circles indicate the presence of the Eigen core cation. Distances are in angstroms.

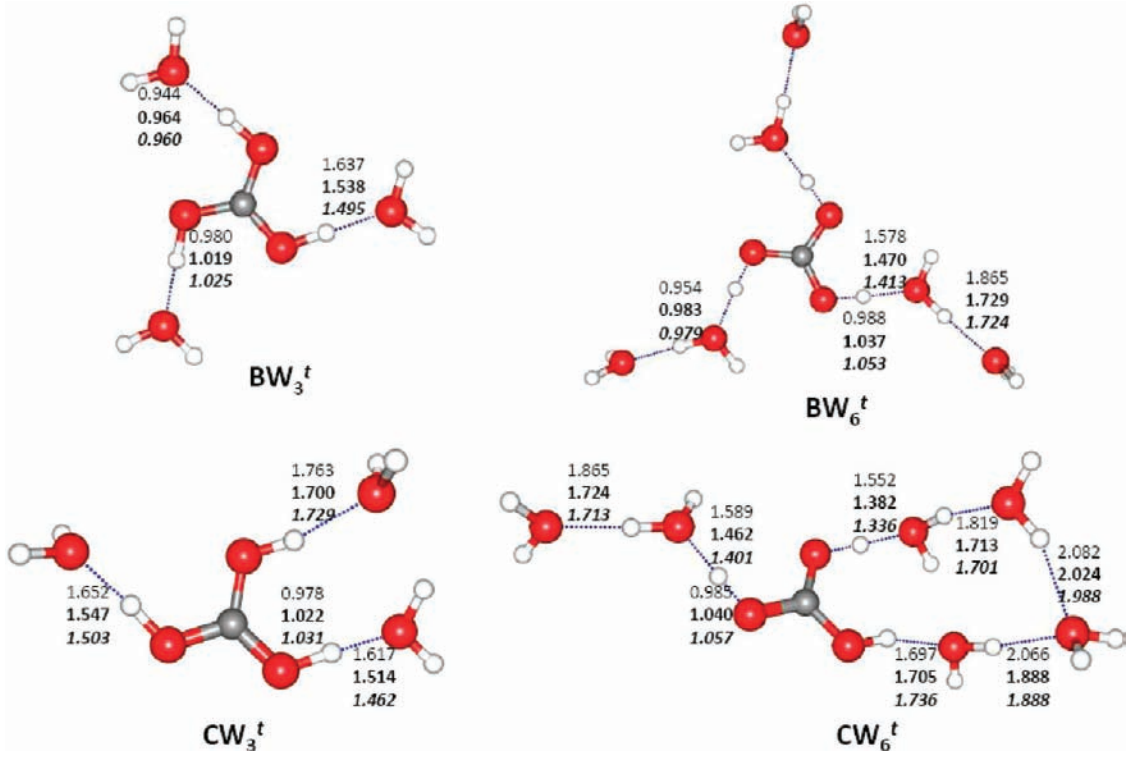

Figure 8. Optimized geometries of BW_n^t and CW_n^t trihydroxy clusters (where $n = 3$ and 6) at the HF/6-311++G** (normal), B3LYP/6-311++G** (bold), and M05-2X/6-311++G** (bold and italic) levels of theory. Distances are in angstroms.

parameters indicates that the M05-2X/6-311++G** method yields shorter O−H···O distances than the B3LYP and HF methods. The general trend in the O−H···O distance obtained using the 6-311++G** basis set is M05-2X < B3LYP < HF.

TABLE 1: Sequential Binding Energies (kJ/mol) Calculated at the B3LYP/6-311++G Level for $PCAW_n^x$ Clusters[a], along with Calculated and Experimental Values for Corresponding Clusters with Monovalent Lithium Cation (Li^+)**

	isomer A			isomer B		isomer C		SBE of $Li^+(H_2O)_n$	
n	linear (l)	branched (b)	cyclic (c)	mono (m)	di (d)	mono (m)	di (d)	calc[b]	expt[c]
1	148	–	–	127	–	122	128	149	142
2	106	104	–	103	100	103	106	127	108
3	71	68	105	71	75	71	90	96	86
4	63	60	77	61	63	61	83	65	69
5	51	49	57	51	51	50	57	59	58
6	48	47	51	48	46	47	64	55	51

[a] $PCAW_n^x$, where $n = 1-6$; $x =$ l, b, c, m, and d. [b] Calculated SBE value taken from ref 42 obtained at the B3LYP/6-311++G** level. [c] Experimental value taken from ref 50.

However, in clusters BW_2^d, BW_4^{d2}, and BW_6^{d3}, there is no similar trend. Evidence from the present calculations reveals that, among the three methods, B3LYP and M05-2X yield consistent geometries.

3.5. Energetics of $PCAW_n^x$ Clusters ($n = 1-6$ and $x =$ l, b, c, m, d, and t). SBEs of ion solvation are important quantities that can be measured experimentally. The experimental and theoretical values of SBEs of monovalent cation such as Li^+, Na^+, and K^+ with water have been reported.[42a] In a previous study, the B3LYP/6-311++G** level of calculation was used to compute the trends in the SBEs of monovalent metal cations.[42a] The same method was selected here to calculate the SBEs of $PCAW_n^x$ clusters ($n = 1-6$). The BSSE-corrected SBEs for various clusters are presented in Table 1. Close scrutiny of the results reveals that the addition of the first water molecule to PCA requires more energy than the addition of subsequent water molecules. The incremental SBE gradually decreases with the stepwise addition of water molecules, except in the case of dihydroxy clusters of isomer C (CW_n^d). This might be due to the changes in the H-bonding pattern in linear and cyclic clusters. It can be seen from Figure 7 that CW_5^d contains an additional water molecule in the first solvation shell and has the Eigen cation localized at a different position compared to the same in CW_4^d and CW_6^d. The general trend observed from this study is similar to that of previous investigation on the solvation of mono- and divalent metal cations.[42] The calculated ranges of SBEs for isomers A, B, and C are 47−148, 46−127, and 47−128 kJ/mol, respectively. The corresponding energies for the monovalent cations obtained from various experimental[50] and theoretical[42] studies are in the ranges 51−142 and 55−149 kJ/mol, respectively. It is interesting to note that the calculated ranges of SBEs of isomers A−C are similar to the Li^+.

The BSSE-corrected BEs of different $PCAW_n^x$ clusters of isomers A−C are listed in Tables 2−4. The BSSE-corrected BEs of $PCAW_n^x$ clusters calculated using the HF method with the 6-31+G*and 6-311++G** are provided in the Supporting Information (Table S1). It can be seen that the BE increases with increasing degree of solvation. However, the incremental BE decreases increasing number of water molecules in the cluster. As an example, the incremental BE of AW_2^l with respect to AW_1^l is 34.6 kcal/mol at the M05-2X/6-311++G** level of calculations, whereas the same for AW_3^l with respect to AW_2^l is 19.1 kcal/mol. A similar trend has also been observed in the hydration of Eigen and Zundel cations.[51]

It can be seen from the optimized geometries that isomer A prefers to form linear, branched, and cyclic clusters. Among these clusters, BE values of linear protonated wire-type clusters of isomer A are higher than those for the branched and cyclic types. Both B and C isomers form mono-, di-, and trihydroxy clusters. Comparison of BEs of these clusters shows that dihydroxy clusters are more stable than the other types. Even though cyclic clusters are observed by isomer C, a linear hydration pattern is more favorable than the other types for this isomer. A comparison of the BEs of corresponding water clusters for all isomers reveals that AW_1^l, CW_2^m, BW_3^d, BW_4^{d1}, BW_5^{d2}, and BW_6^{d3} are more stable than the other clusters with same numbers of water molecules.

TABLE 2: Binding Energies (kcal/mol) of Isomer A Clusters (AW_n^x, where $n = 1-6$; $x =$ l, b, and c) Calculated by the B3LYP and M05-2X Methods Using the 6-31+G* and 6-311++G Basis Sets**

	B3LYP		M05-2X	
	6-31+G*	6-311++G**	6-31+G*	6311++G**
AW_1^l	34.6	**35.4**	38.8	**39.5**[a]
AW_2^l	68.8	70.5	71.8	74.2
AW_3^l	88.0	88.3	91.3	93.4
AW_4^l	100.0	101.1	105.0	107.5
AW_5^l	112.9	114.8	118.3	121.4
AW_6^l	124.4	125.5	130.5	133.8
AW_2^b	54.6	55.5	56.4	58.6
AW_3^b	73.6	74.5	79.2	80.7
AW_4^b	86.5	87.4	91.1	93.4
AW_5^b	100.4	100.8	106.7	108.3
AW_6^b	110.6	111.5	117.1	119.7
AW_3^c	85.9	85.7	91.1	90.6
AW_4^c	98.7	98.9	108.6	110.0
AW_5^c	112.4	112.2	117.0	122.2
AW_5^{c1}	99.8	99.9	106.1	107.0
AW_6^c	118.6	124.6	129.8	131.3

[a] BEs corresponding to the most stable clusters among isomers A−C given in bold.

It can be noted that the basis sets have a marginal effect on the calculated BEs of various hydrated clusters. However, the inclusion of electron correlation has a considerable effect on the calculated BEs. BEs of various clusters obtained from M05-2X calculations are higher than the corresponding B3LYP values. This might be due to the improved treatment of intermolecular interactions at the M05-2X level of theory. The importance of the correlation energy in the BEs was assessed by computing the differences in BEs obtained from HF calculations compared to B3LYP and M05-2X calculations. The difference in the BEs was taken as the electron correlation contribution. The results are presented in Table S2 of the Supporting Information. The percentage of electron correlation energy contributed to the BE at the M05-2X level of calculation for various clusters ranges from 15% to 50%. These results confirm that electrostatic interactions contribute significantly to the stability of various clusters in addition to the dispersive interaction. Table S2 (Supporting Information) shows that the percentage electron correlation contribution to the BE is higher for the M05-2X method than for the B3LYP method. As explained by Truhlar and co-workers, the parameters used in

TABLE 3: Binding Energies (kcal/mol) of Isomer B Clusters (BW_n^x, where $n = 1-6$, x = m, d, and t) Calculated by the B3LYP and M05-2X Methods Using the 6-31+G* and 6-311++G Basis Sets**

	B3LYP		M05-2X	
	6-31+G*	6-311++G**	6-31+G*	6311++G**
BW_1^m	29.3	30.4	33.0	34.3
BW_2^m	69.6	71.5	72.9	75.3
BW_3^m	88.8	89.3	93.6	93.6
BW_4^m	100.9	101.7	105.2	106.7
BW_5^m	119.3	116.4	121.9	122.0
BW_6^m	124.0	124.9	130.5	132.9
BW_2^d	49.2	50.4	52.3	55.2
BW_3^d	86.7	**110.9**	103.7	**115.0**[a]
BW_4^{d1}	102.9	**104.9**	107.9	**111.5**
BW_4^{d2}	83.6	84.7	91.6	93.8
BW_5^{d1}	121.8	121.3	123.4	126.4
BW_5^{d2}	117.2	**120.9**	124.5	**129.4**
BW_5^{d3}	97.3	97.6	106.7	107.9
BW_6^{d1}	126.1	127.7	133.3	136.3
BW_6^{d2}	130.4	131.8	135.7	139.8
BW_6^{d3}	130.9	**132.3**	142.1	**146.9**
BW_6^{d4}	128.8	131.5	126.4	143.1
BW_3^t	66.4	67.4	70.1	72.8
BW_6^t	107.8	108.3	117.2	118.8

[a] BEs corresponding to the most stable clusters among isomers A−C given in bold.

TABLE 4: Binding Energies (kcal/mol) of Isomer C Clusters (CW_n^x, where $n = 1-6$, x = m, d, and t) Calculated by the B3LYP and M05-2X Methods Using the 6-31+G* and 6-311++G Basis Sets**

	B3LYP		M05-2X	
	6-31+G*	6-311++G**	6-31+G*	6311++G**
CW_1^m	28.4	29.1	31.6	32.8
CW_2^m	71.6	**73.2**	75.3	**77.1**[a]
CW_3^m	90.8	91.3	95.3	94.9
CW_4^m	101.4	102.6	106.0	108.2
CW_5^m	116.6	116.8	121.9	123.4
CW_6^m	125.2	126.2	131.1	133.5
CW_1^d	31.1	30.7	32.8	32.5
CW_2^d	51.5	51.4	55.5	56.2
CW_3^d	68.7	69.0	73.5	75.6
CW_4^d	95.4	95.4	100.5	101.6
CW_5^d	109.4	109.7	120.2	119.0
CW_6^d	121.5	121.8	129.4	130.9
CW_3^t	69.0	68.8	72.9	74.2
CW_6^t	113.1	112.5	123.9	123.9

[a] BEs corresponding to the most stable clusters among isomers A−C given in bold.

the M05-2X method are generated by the simultaneous optimization of exchange and correlation functionals with the kinetic energy density included in both of them, so that an improved treatment of medium-range correlation effects is obtained by this exchange-correlation functional.[43,44]

Some of the problems encountered in deriving thermochemical parameters for hydrated clusters using static quantum chemical calculations include the floppiness of the molecules involved and the existence of many isomers with small energy differences. However, static quantum chemical calculations can provide useful trends. The thermochemical parameters were calculated for the structures obtained from geometry optimization at the B3LYP/6-31+G* level using the methodology

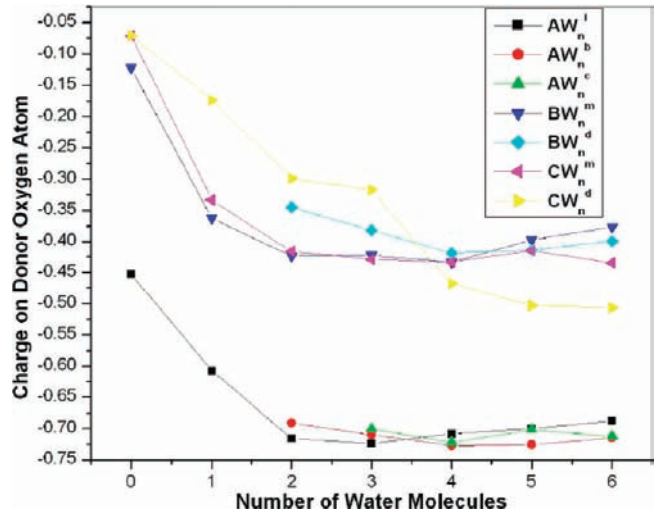

Figure 9. Correlation of the number of water molecules in $PCAW_n^x$ (isomers A, B, and C) versus total Mullikan charge on the proton-donating oxygen atoms in the clusters at the M05-2X/6-311++G** level.

implemented in the Gaussian package. The calculated thermodynamic parameters at 298 K for various hydrated clusters are presented in Table S3 of the Supporting Information. The calculated free energy values reveal that hydration of PCA is favorable in general and, in particular, dihydroxy hydration of isomer C is more favorable than hydration of isomers B and A.

3.6. Charge Analysis. Charges on the proton-donating oxygen atom of isomers A−C and their hydrated clusters were obtained from Mulliken population analysis (MPA). The variation of the charge with the number of water molecules is plotted in Figure 9. The charge on the proton-donor oxygen decreases as a result of proton transfer. For linear clusters (AW_n^l), the charge on the oxygen atom decreases dramatically up to $n = 3$, and thereafter, the variation in the charge is constant. These results show that proton movement is localized in the middle of the linear chain, which is in accordance with the findings of an earlier report.[33b] A similar trend can be seen from the plot for monohydroxy clusters of isomers B and C.

3.7. Vibrational Frequencies. Recent developments in spectroscopic measurements and theoretical calculations have successfully unveiled structures of protonated water clusters.[21,52−58] Scaled vibrational frequencies of all of the hydrated clusters studied here, calculated at the B3LYP/6-31+G* level of theory using the harmonic approximation, are listed in Tables 5−7. Both experimental and theoretical vibrational frequencies of protonated water clusters from previous studies[21c,55] are included as reference for analysis of the values for $PCAW_n^x$ clusters.

It was found in previous experimental studies that the asymmetric (E_{as}) and symmetric (E_{ss}) stretching frequencies of bare H_3O^+ are 3530 and 3390 cm^{-1}, respectively.[59] The corresponding values calculated in the present investigation using the B3LYP/6-31+G* method are 3508 and 3414 cm^{-1}, which are in good agreement with the above-mentioned experimental values. In protonated water clusters, these E_{as} and E_{ss} modes occur at 2665 and 2420 cm^{-1}, respectively, because of H-bonding.[21c,55] In addition, H−O−H bending modes of the Eigen core (major component) and dangling water molecules (minor component) are found at 1900 and 1760 cm^{-1}.[21c,55] In the same study, the H−O−H intramolecular bend of dangling water molecules was observed at 1620 cm^{-1}. Spectral features

TABLE 5: Calculated OH-Stretching Frequencies of the Eigen (E) Core Present in AW_n^x Clusters[a] at the B3LYP/6-31+G* Level along with Experimental Values from Protonated Water Clusters

AW_n^x	description of OH stretching[b,c]	ν_{calc} (cm^{-1})	ν_{expt}[d] (cm^{-1})
H_3O^+	E_{as}	3508	3530[e]
	E_{ss}	3414	3390[f]
isomer A	E_{as}	3568	3566[g]
	E_{ss}	3497	3545[g]
	H-bonded O−H stretch to CO_2	2863	2869[g]
AW_1^l	H-bonded O−H stretch to CO_2	3320	
	E-core free −OH stretch	3615	3580
	H−O−H bend of E core and dangling H_2O	1958	1900, 1760
AW_2^l	E-core stretching	2066	∼2100
	E_{as}	2616	2665
AW_3^l	E_{as} stretch to AD-type H_2O[e]	2660	2665
	$O-H^+-O$ stretching mode	1302	1317[h], 1337[i]
AW_4^l	H−O−H bend of E core and dangling H_2O	1908	1900
	E_{ss} stretch to AD-type H_2O[e]	2228	2420
	E-core free −OH stretch	3652	3580
AW_5^l	$O-H^+-O$ bending mode	1465	∼1510[j]
	H−O−H bend of E core and dangling H_2O	1802	1900
	E_{ss} stretch to AD-type H_2O	2261	2420
AW_6^l	H−O−H bend of E core and dangling H_2O	1821	1900
	E_{ss} stretch to AD-type H_2O	2078	2420
AW_2^b	E_{as}	2525	2665
	E-core stretch to A-type H_2O	2715	2830[anh k]
	H-bonded O−H stretch with CO_2	3446	
AW_3^b	H−O−H bend of E core and dangling H_2O	1891	1900
	E-core HB stretch to A-type H_2O	2913	2889[anh]
	AD-type H_2O H-bond stretch	3200	3195
AW_4^b	E_{as} stretch to AD-type H_2O	2202	2665
	E_{ss} stretch to AD-type H_2O	2364	2420
AW_5^b	H−O−H bend of E core and dangling H_2O	1826	1900
	E_{as} stretch to AD-type H_2O	2600	2665
AW_6^b	E-core stretch to AD-type H_2O	1996	1885
	E_{ss} to AD-type H_2O	2282	2420
AW_3^c	H−O−H bend of E core and dangling H_2O	1852	1900
	E_{as} stretch to AD-type H_2O	2605	2665
AW_4^c	$O-H^+-O$ bending mode	1470	∼1510[j]
	E-core HB stretch to A-type H_2O	3030	2889
AW_5^c	E_{as} stretch to ADD-type H_2O	2730	2665
	E_{ss} to AD-type H_2O	2388	2420
AW_5^{c1}	E-core stretching	2111	2100
	E_{ss}	2360	2420
AW_6^c	E-core dangling H_2O	2225	2100
	E_{as} stretch to AD-type H_2O	2613	2665

[a] AW_n^x clusters, where $n = 1-6$, $x =$ l, b, and c, use harmonic calculations (B3LYP with 6-31+G* basis set) and are scaled by 0.973. [b] E, Eigen cation; PCA, protonated carbonic acid; CA, carbonic acid; E_{as}, Eigen asymmetric stretch; E_{ss}, Eigen symmetric stretch. [c] A-type H_2O molecules accept a hydrogen bond from the Eigen core. AD-type H_2O molecules accept and donate a hydrogen-bond. ADD-type H_2O molecules accept one and donate two hydrogen bonds (HBs). [d] Unless otherwise indicated, experimental O−H stretching frequencies of protonated water clusters taken from refs 21c and 55. [e] Taken from ref 59a. [f] Taken from ref 59b. [g] Experimental O−H stretching frequency value taken from ref 15. [h] Taken from ref 53. [i] Taken from ref 54. [j] Taken from ref 57. [k] anh, anharmonic frequencies.

of Zundel cations reported in protonated water cluster appear in the range of 600−1900 cm^{-1}. Asmis et al. reported an $O-H^+-O$ stretching mode at 1317 cm^{-1} in protonated water clusters.[53] Fridgen and co-workers observed the same band at 1337 cm^{-1}.[54] Recently, very weak $O-H^+-O$ bending frequencies (∼1510 and ∼1370 cm^{-1}) were reported.[57] The same study provided evidence for the existence of an $(O-H^+-O)_{as}$ stretching frequency at ∼1000 cm^{-1}.[57] This spectral information was used as the basis for analysis of the vibrational spectral frequencies of $PCAW_n^x$ clusters.

Tables 5−7 reveal the presence of vibrational frequencies in the ranges of 2202−2730 and 2078−2566 cm^{-1} in $PCAW_n^x$ clusters. A comparison of these values with those of protonated water clusters reveals that these signals can be assigned to the E_{as} and E_{ss} modes of the Eigen cation. Analysis of the results indicates the presence of the Eigen core in all clusters except in the case of trihydroxy hydrated clusters. The calculated asymmetric (E_{as}) and symmetric (E_{ss}) stretching frequencies of free O−H of the Eigen core in isomer A are 3568 and 3497 cm^{-1}, respectively. The corresponding experimental values for the same obtained from IR photodissociation (IRPD) studies[15] on PCA are 3566 and 3545 cm^{-1}. The calculated stretching frequency of the O−H group that is H-bonded to the CO_2 fragment of isomer A is 2863 cm^{-1}, which is in close agreement with the experimental value of 2869 cm^{-1}.[15] In AW_1^l, the free O−H stretching frequency of the Eigen core occurs at 3615 cm^{-1}. In the same cluster, a value of 1958 cm^{-1} has been observed. This might be due to the H−O−H bend of the Eigen core and dangling water molecules, in accordance with a previous report.[21c,55]

In AW_2^l, the O−H stretching frequencies of the Eigen core occur at 2066 (2100) and 2616 (2665) cm^{-1}. The calculated E_{as} frequency of the AW_3^l cluster is 2660 cm^{-1}. These values are in close agreement with the respective experimental frequencies of protonated water clusters. The calculated $O-H^+-O$ stretching mode in the AW_3^l cluster is observed at 1302 cm^{-1}. The corresponding experimental value for protonated water clusters varies from 1317 to 1337 cm^{-1}. It is interesting to see that all of the clusters with isomer A have spectral signatures of the Eigen core. As mentioned, the spectral features in the lower-energy region below 1900 cm^{-1} might arise as a result of Eigen-to-Zundel and Zundel-to-Eigen transitions during proton transport. Although geometrical parameters obtained form the present static quantum chemical calculations do not provide any signatures of Zundel ions, the calculated vibrational frequencies in the lower-energy region yield some clues about the involvement of Zundel ions during proton transfer.

It is well-known that the vibrational frequencies of individual molecules undergo a considerable red shift upon formation of H-bonded complexes, and the same type of red shift has been used to characterize the H-bonding interactions in protonated water clusters. Analysis of all of the values listed in the tables reveals larger red shifts (∼790−2600 cm^{-1}) and higher intensity values (∼2000−6000 arbitrary units) in all of the clusters. Similar observations (very large red shifts of ∼1100−1630 cm^{-1} and intensities of ∼3000−5000 arbitrary units) have been made in earlier experimental[21] and theoretical studies on hydrated Eigen or Zundel ions.[52−58]

The experimental and calculated O−H stretching frequencies of isomer B are 3520 and 3511 cm^{-1}, respectively.[15] It may ne noticed from Table 6 that the O−H stretching frequency of BW_1^m, which is H-bonded to a water molecule, is 2022 cm^{-1} and the corresponding red shift is 1489 cm^{-1}. The stretching of free O−H occurs at 3545 cm^{-1}. The $O-H^+-O_{as}$ stretching modes of clusters BW_5^m and BW_3^d occur at 869 and 860 cm^{-1}, respectively. This is due to the

TABLE 6: Calculated OH-Stretching Frequencies of the Eigen (E) Core Present in BW_n^x Clusters[a] at the B3LYP/6-31+G* Level along with Experimental Values from Protonated Water Clusters

BW_n^x	description of O−H stretching[b]	ν_{calc} (cm^{-1})	ν_{expt}[c] (cm^{-1})
isomer B	$O-H_{ss}$	3511	3520[d]
BW_1^m	PCA O−H stretch to A-type H_2O (corresponding red shift, 1489 cm^{-1})	2022	
	free O−H stretching in PCA	3545	
BW_2^m	E-core stretching	2148	∼2100
	E_{as}	2636	2665
	E-core free −OH stretch	3629	3580
BW_3^m	$O-H^+-O$ stretching mode	1300	1317,[e] 1337[f]
	H−O−H bend	1723	1756,[e] 1768
	E-core H-bond stretch to CA ($CA\cdots H_3O^+$)	2747	2730[h]
BW_4^m	$O-H^+-O$ stretching mode	1417	1317,[e] 1337[f]
	E_{ss} to AD-type H_2O	2414	2420
BW_5^m	$O-H^+-O_{as}$ stretching mode	869	921,[e] 990,[f] 1000[g]
	E_{ss} to AD-type H_2O	2566	2420
BW_6^m	$O-H^+-O$ stretching mode	1441	1317,[e] 1337[f]
	E_{ss} to AD-type H_2O	2160	2420
BW_2^g	CA O−H stretch to A-type H_2O (corresponding red shift, 1055 cm^{-1})	2456	
BW_3^g	$O-H^+-O_{as}$ stretching mode	860	921,[e] 990,[f] 1000[g]
	CA O−H stretch to A-type H_2O	2839	
BW_4^{d1}	H−O−H bend of E core and dangling H_2O	1994	1900
	E_{ss} stretch to AD-type H_2O	2324	2420
	CA O−H stretch to A-type H_2O	2974	
BW_4^{d2}	PCA O−H stretch to AD-type H_2O (corresponding red shift, 1589 cm^{-1})	1922	
BW_5^{d1}	$O-H^+-O$ stretching mode	1039	1043,[e] 1000[g]
	E_{ss} stretch to AD-type H_2O	2548	2420
	CA O−H stretch to A-type H_2O	3064	
BW_5^{d2}	H−O−H bend of E core and dangling H_2O	1951	1900
	E_{ss} stretch to AD-type H_2O	2318	2420
	CA O−H stretch to AD-type H_2O	2552	
BW_5^{d3}	PCA O−H stretch to AD-type H_2O	1368 and 2038	
BW_6^{d1}	H−O−H bend of E core and dangling H_2O	1842	1900
	E_{ss} stretch to AD-type H_2O	2100	2420
	CA O−H stretch to A-type H_2O	3085	
BW_6^{d2}	$O-H^+-O$ stretching mode	1458	1317,[e] 1337[f]
	E_{ss} to AD-type H_2O	2373	2420
	CA O−H stretch to AD-type H_2O	2673	
BW_6^{d3}	$O-H^+-O$ stretching mode	1326	1317[e], 1337[f]
	PCA O−H stretch to AD-type H_2O (corresponding red shift, 1326 cm^{-1})	2185	
BW_6^{d4}	PCA O−H stretch to AD-type H_2O	1490 and 2536	
	H−O−H bend of E core and dangling H_2O	1960	1900
	E_{ss}	2243	2420
BW_3^t	PCA O−H stretch to A-type H_2O (corresponding red shifts, 805 and 801 cm^{-1})	2706 and 2710	
BW_6^t	PCA O−H stretch to AD-type H_2O (corresponding red shifts, 1169 and 1150 cm^{-1})	2342 and 2361	

[a] BW_n^x clusters, where $n = 1-6$, x = m, d, and t, use harmonic calculations (B3LYP with 6-31+G* basis set) and are scaled by 0.973. [b] E, Eigen cation; PCA, protonated carbonic acid; CA, carbonic acid; $O-H_{ss}$, O−H symmetric stretching; E_{as}, Eigen asymmetric stretch; E_{ss}, Eigen symmetric stretch. [c] Unless otherwise indicated, experimental O−H stretching frequencies of protonated water clusters taken from refs 21c and 55. [d] Experimental O−H stretching frequency value taken from ref 15. [e] Taken from ref 53. [f] Taken from ref 54. [g] Taken from ref 57. [h] Taken from ref 58b.

oscillation of the proton between the two water molecules. The presence of the Eigen core in clusters BW_n^m ($n = 2-6$) and BW_n^d ($n = 4-6$) is evident from the spectral information. It is necessary to mention that BW_n^d clusters with unequal numbers of water molecules have the geometric and spectral signatures of the Eigen core. Vibrational frequencies of lower-energy modes are presented in monohydroxy clusters (BW_n^m, where $n = 3-6$) and dihydroxy clusters (BW_3^d, BW_5^{d1}, BW_5^{d3}, BW_6^{d2}, BW_6^{d3}, and BW_6^{d4}).

The calculated O−H stretching frequencies of CW_n^x clusters are presented in Table 7. The O−H stretching frequency of isomer C is 3556 cm^{-1}. In CW_1^m, the O−H stretching frequency is 2122 cm^{-1}. The corresponding red shift is 1434 cm^{-1}. The O−H stretching frequencies and Eigen signatures of CW_n^x clusters are analogous to those of BW_n^x clusters. Vibrational frequencies of lower-energy modes are presented in monohydroxy clusters only (CW_n^m, where $n = 3$, 5, and 6). It can be seen that fully hydrated Eigen cores are present in AW_5^c, AW_5^{c1}, AW_6^c, CW_4^d, CW_5^d, and CW_6^d. These O−H stretching frequen-

TABLE 7: Calculated OH-Stretching Frequencies of the Eigen (E) Core Present in CW_n^x Clusters[a] at the B3LYP/6-31+G* Level along with Experimental Values from Protonated Water Clusters

CW_n^x	description of O−H stretching[b]	ν_{calc} (cm^{-1})	ν_{expt}[c] (cm^{-1})
isomer C	$O-H_{ss}$	3556	
CW_1^m	PCA O−H stretch to A-type H_2O (corresponding red shift, 1434 cm^{-1})	2122	
	free O−H stretching in PCA	3618	
CW_2^m	E-core stretching	2180	∼2100
	E_{as}	2615	2665
	E-core free −OH stretch	3638	3580
CW_3^m	$O-H^+-O$ stretching mode	1281	1317,[d] 1337[e]
	H−O−H bend	1753	1756,[d] 1768
	E-core H-bond stretch to CA ($CA\cdots H_3O^+$)	2794	2730[g]
CW_4^m	H−O−H bend of E core and dangling H_2O	1901	1900
	E_{ss} to AD-type H_2O	2271	2420
CW_5^m	$O-H^+-O$ stretching mode	1232	1317,[d] 1337[e]
	H−O−H bend	1761	1756,[d] 1768
	E_{ss} to AD-type H_2O	2432	2420
CW_6^m	$O-H^+-O$ stretching mode	1508	1317,[d] 1337[e]
	H−O−H bend of E core and dangling H_2O	1805	1900
	E-core stretching	2090	∼2100
CW_1^f	PCA O−H stretch to AA-type H_2O	3279	
	free O−H stretching in PCA	3563	
CW_2^d	PCA O−H stretch to A-type H_2O (corresponding red shifts, 1135 and 611 cm^{-1})	2421 and 2945	
CW_3^d	PCA O−H stretch to AD-type H_2O (corresponding red shift, 935 cm^{-1})	2621	
CW_4^d	H−O−H bend	1806	1756,[d] 1768
	E_{as}	2501	2665
	E-core stretch to CA and AD-type H_2O	2754	
CW_5^d	E-core stretching	2198	∼2100
	E_{ss} to AAD-type H_2O	2438	2420
CW_6^d	E_{ss} to AD-type H_2O	2308	2420
	E-core stretch to CA and AD-type H_2O	2715	2730[g]
	E-core stretch to AAD-type H_2O	3125	
CW_3^t	PCA O−H stretch to A-type H_2O (corresponding red shifts, 900 and 444 cm^{-1})	2656 and 3112	
CW_6^t	PCA O−H stretch to AD-type H_2O (corresponding red shifts, 1670 and 1158 cm^{-1})	1886 and 2398	

[a] CW_n^x clusters, where $n = 1-6$, $x =$ m, d, and t, use harmonic calculations (B3LYP with 6-31+G* basis set) and are scaled by 0.973. [b] E, Eigen cation; PCA, protonated carbonic acid; CA, carbonic acid; $O-H_{ss}$, O−H symmetric stretching; E_{as}, Eigen asymmetric stretch; E_{ss}, Eigen symmetric stretch. [c] Unless otherwise indicated, experimental O−H stretching frequencies of protonated water clusters taken from refs 21c and 55. [d] Taken from ref 53. [e] Taken from ref 54. [f] Taken from ref 57. [g] Taken from ref 58b.

cies of the Eigen core are in good agreement with the available experimental and theoretical values for protonated water clusters.[21,52−58]

4. Summary and Conclusions

In this study, an attempt has been made to probe the sequential hydration of three different isomers of PCA. The geometrical parameters of clusters reveal the occurrence of proton transfer from PCA to water in linear and monohydroxy hydrated clusters. The presence of the Eigen core in proton transfer is evident from the geometries and IR spectral signatures of these clusters. The lower-energy modes illustrate the involvement of Eigen → Zundel → Eigen transitions in proton transfer in $PCAW_n^x$ clusters. One of the important results emerging from the present study is that the symmetrically hydrated clusters do not favor proton transport. The SBEs of all of the clusters are similar to those for the hydration of the Li^+ ion. Comparison of BEs of all of the clusters containing a single water molecule reveals that the AW_1^l cluster has the maximum stability. In clusters with two water molecules, monohydroxy hydrated isomer C has the highest stability. For $n = 3-6$, the clusters of isomer B, viz., BW_3^d, BW_4^{d1}, BW_5^{d2}, and BW_6^{d3} have the maximum BEs when compared to the respective clusters of isomers A and C with the same numbers of water molecules. The calculated BEs indicate that the electrostatic interaction is the predominant interaction in the stabilization of these clusters and the contribution of intermolecular dispersive interaction (correlation energy) at M05-2X/6-311++G** varies from 15% to 50% depending on the intrinsic nature of the clusters.

Acknowledgment. We thank the Council of Scientific and Industrial Research (CSIR), New Delhi, India, for financial support. SRG is thankful to the Department of Science and Technology (DST), New Delhi for the award of J. C. Bose Fellowship to him. The authors also thank the anonymous reviewers for their valuable comments and suggestions.

Supporting Information Available: BEs calculated by the HF method, contribution of electron correlation to the BEs, and thermochemical parameters of $PCAW_n^x$ clusters are given Tables S1−S3. The starting and final optimized geometries of AW_n clusters (where $n = 1$, 3, and 6) are provided in Figure S1. This material is available free of charge via the Internet at http://pubs.acs.org.

References and Notes

(1) Pocker, Y.; Bjorkquist, D. W. *J. Am. Chem. Soc.* **1977**, *99*, 6537.
(2) Nguyen, M. T.; Ha, T. K. *J. Am. Chem. Soc.* **1984**, *106*, 599.
(3) Marlier, J. F.; O'Leary, M. H. *J. Am. Chem. Soc.* **1984**, *106*, 5054.
(4) Liang, J. Y.; Lipscomb, W. N. *J. Am. Chem. Soc.* **1986**, *108*, 5051.
(5) Mertz, K. M. *J. Am. Chem. Soc.* **1990**, *112*, 7973.
(6) Liedl, K. R.; Sekusak, S.; Mayer, E. *J. Am. Chem. Soc.* **1997**, *119*, 3782.
(7) Ludwig, R.; Kornath, A. *Angew. Chem., Int. Ed.* **2000**, *39*, 1421.
(8) Al-Hosney, H. A.; Grassian, V. H. *J. Am. Chem. Soc.* **2004**, *126*, 8068.
(9) Tossell, J. A. *Geochim. Cosmochim. Acta* **2005**, *69*, 5647.
(10) Al-Hosney, H. A.; Grassian, V. H. *Phys. Chem. Chem. Phys.* **2005**, *7*, 1266.
(11) (a) Kumar, P. P.; Kalinichev, A. G.; Kirkpatrick, R. J. *J. Chem. Phys.* **2007**, *126*, 204315. (b) Nguyen, M. T.; Matus, M. H.; Jackson, V. E.; Ngan, V. T.; Rustad, J. R.; Dixon, D. A. *J. Phys. Chem. A* **2008**, *112*, 10386. (c) Kumar, P. P.; Kalinichev, A. G.; Kirkpatrick, R. J. *J. Phys. Chem. B* **2009**, *113*, 794.
(12) Jena, N. R.; Mishra, P. C. *Theor. Chem. Acc.* **2005**, *114*, 189.
(13) Hage, W.; Liedl, K. R.; Hallbrucker, A.; Mayer, E. *Science* **1998**, *279*, 1332.
(14) (a) Wight, C. A.; Boldyrev, A. I. *J. Phys. Chem.* **1995**, *99*, 12125. (b) Nguyen, M. T.; Raspoet, G.; Vanquickenborne, L. G.; Van-Duijnen, P. T. *J. Phys. Chem. A* **1997**, *101*, 7379. (c) Loerting, T.; Tautermann, C.; Kroemer, R. T.; Kohl, I.; Hallbrucker, A.; Mayer, E.; Liedl, K. R. *Angew. Chem., Int. Ed.* **2000**, *39*, 892. (d) Lewis, M.; Glaser, R. *J. Phys. Chem. A* **2003**, *107*, 6814.
(15) Andrei, H. S.; Nizkorodov, S. A.; Dopfer, O. *Angew. Chem., Int. Ed.* **2007**, *46*, 4754.
(16) (a) Egsgaard, H.; Carlsen, L. *J. Chem. Soc., Faraday Trans. I* **1989**, *85*, 3403. (b) Gerbaux, P.; Turecek, F. *J. Phys. Chem. A* **2002**, *106*, 5938.
(17) (a) Bieske, E. J.; Dopfer, O. *Chem. Rev.* **2000**, *100*, 3963. (b) Roth, D.; Dopfer, O. *Phys. Chem. Chem. Phys.* **2002**, *4*, 4855.
(18) (a) Olah, G. A.; White, A. M. *J. Am. Chem. Soc.* **1968**, *90*, 1884. (b) Olah, G. A. *Science* **1970**, *168*, 1298. (c) Rasul, G.; Reddy, V. P.; Zdunek, L.; Prakash, G. K. S.; Olah, G. A. *J. Am. Chem. Soc.* **1993**, *115*, 2236. (d) Minkwitz, R.; Schneider, S. *Angew. Chem., Int. Ed.* **1999**, *38*, 714.
(19) Chiavarino, B.; Crestoni, M. E.; Fornarini, S.; Lanucara, F.; Lemaire, J.; Maitre, P. *Chem. Phys. Chem.* **2009**, *10*, 520.
(20) (a) Nagle, J. F.; Nagle, S. T. *J. Membr. Biol.* **1983**, *74*, 1. (b) Tuckerman, M.; Laasonen, K.; Sprik, M.; Parinello, M. *J. Chem. Phys.* **1995**, *103*, 150. (c) Chou, T. *J. Phys. Chem. A* **2002**, *35*, 4515. (d) Pang, X. F.; Feng, Y. P. *Chem. Phys. Lett.* **2003**, *373*, 392. (e) Iannuzzia, M. *J. Chem. Phys.* **2006**, *124*, 204710. (f) Hassana, S. A. *J. Chem. Phys.* **2006**, *124*, 204510.
(21) (a) Miyazaki, M.; Fujii, A.; Ebata, T.; Mikami, N. *Science* **2004**, *304*, 1134. (b) Shin, J. W.; Hammer, N. I.; Diken, E. G.; Johnson, M. A.; Walters, R. S.; Jaeger, T. D.; Duncan, M. A.; Christie, R. A.; Jordan, K. D. *Science* **2004**, *304*, 1137. (c) Headrick, J. M.; Diken, E. G.; Walters, R. S.; Hammer, N. I.; Christie, R. A.; Cui, J.; Myshakin, E. M.; Duncan, M. A.; Johnson, M. A.; Jordan, K. D. *Science* **2005**, *308*, 1765.
(22) Eigen, M. *Angew. Chem., Int. Ed. Engl.* **1964**, *3*, 1.
(23) Zundel, G.; Metzer, H. *Z. Phys. Chem.* **1968**, *58*, 225.
(24) (a) Pome's, R.; Roux, B. *Biophys. J.* **1996**, *71*, 19. (b) Sadeghi, R. R.; Cheng, H. P. *J. Chem. Phys.* **1999**, *111*, 2086. (c) Day, T. J. F.; Schmitt, U. W.; Voth, G. A. *J. Am. Chem. Soc.* **2000**, *122*, 12027.
(25) Agmon, N. *Chem. Phys. Lett.* **1995**, *244*, 456.
(26) (a) Marx, D.; Tuckerman, M. E.; Hutter, J.; Parrinello, M. *Nature* **1999**, *397*, 601. (b) Voth, G. A. *Acc. Chem. Res.* **2006**, *39*, 143.
(27) Swanson, J. M. J.; Maupin, C. M.; Chen, H.; Petersen, M. K.; Xu, J.; Wu, Y.; Voth, G. A. *J. Phys. Chem. B* **2007**, *111*, 4300.
(28) Schmitt, U. W.; Voth, G. A. *J. Phys. Chem. B* **1998**, *102*, 5547.
(29) Cuma, M.; Schmitt, U. W.; Voth, G. A. *J. Phys. Chem. A* **2001**, *105*, 2814.
(30) Day, T. J. F.; Voth, G. A. *Int. J. Mass. Spectrom.* **2005**, *241*, 197.
(31) Wang, F.; Izvekov, S.; Voth, G. A. *J. Am. Chem. Soc.* **2008**, *130*, 3120.
(32) (a) Nagle, J. F. *J. Bioenerg. Biomembr.* **1987**, *19*, 413. (b) Deamer, D. W. *J. Bioenerg. Biomembr.* **1987**, *19*, 457.
(33) (a) Nagle, J. F.; Morowitz, H. J. *Proc. Nat. Acad. Sci. U.S.A.* **1978**, *75*, 298. (b) Pomès, R.; Roux, B. *J. Phys. Chem.* **1996**, *100*, 2519. (c) Pomès, R.; Roux, B. *Biophys. J.* **1998**, *75*, 33. (d) Mei, H. S.; Tuckerman, M. E.; Sagnella, D. E.; Klein, M. L. *J. Phys. Chem. B* **1998**, *102*, 10446. (e) Decornez, H.; Drukker, K.; Hammes-Schiffer, S. *J. Phys. Chem. A* **1999**, *103*, 289. (f) Isaev, A.; Scheiner, S. *J. Phys. Chem. B* **2001**, *105*, 6420. (g) Schumaker, M. F.; Pomès, R.; Roux, B. *Biophys. J.* **2001**, *80*, 12. (h) Cui, Q.; Karplus, M. *J. Phys. Chem. B* **2003**, *107*, 1071. (i) Wraight, C. A. *Biochim. Biophys. Acta* **2006**, *1757*, 886. (j) Vendrell, O.; Gelabert, R.; Moreno, M.; Lluch, J. M. *J. Phys. Chem. B* **2008**, *112*, 13443. (k) Stoyanov, E. S.; Stoyanova, I. V.; Reed, C. A. *Chem. Eur. J.* **2008**, *14*, 3596.
(34) (a) Mann, D. J.; Halls, M. D. *Phys. Rev. Lett.* **2003**, *90*, 195503. (b) Dellago, C.; Naor, M. M.; Hummer, G. *Phys. Rev. Lett.* **2003**, *90*, 105902. (c) Kolesnikov, A. I.; Zanotti, J. M.; Loong, C. K.; Thiyagarajan, P.; Moravsky, A. P.; Loutfy, R. O.; Burnham, C. J. *Phys. Rev. Lett.* **2004**, *93*, 035503.
(35) Saraste, M. *Science* **1999**, *283*, 1488.
(36) (a) Lanyi, J. K. *J. Phys. Chem. B* **2000**, *104*, 11441. (b) Mathias, G.; Marx, D. *Proc. Nat. Acad. Sci. U.S.A.* **2007**, *104*, 6980.
(37) (a) Akeson, M.; Deamer, D. W. *Biophys. J.* **1991**, *60*, 101. (b) Schumaker, M. F.; Pome's, R.; Roux, B. *Biophys. J.* **2000**, *78*, 2840. (c) Chernyshev, A.; Cukierman, S. *Biophys. J.* **2006**, *91*, 580.
(38) Maupin, C. M.; Saunders, M. G.; Thorpe, I. F.; McKenna, R.; Silverman, D. N.; Voth, G. A. J. *Am. Chem. Soc.* **2008**, *130*, 11399.
(39) Frank, R. A. W.; Titman, C. M.; Pratap, J. V.; Luisi, B. F.; Perham, R. N. *Science* **2004**, *306*, 872.
(40) Mohammed, O. F.; Pines, D.; Dreyer, J.; Pines, E.; Nibbering, E. T. J. *Science* **2005**, *310*, 83.
(41) (a) Loerting, T.; Liedl, K. R. *J. Phys. Chem. A* **2001**, *105*, 5137. (b) Liu, D.; Wyttenbach, T.; Barran, P. E.; Bowers, M. T. *J. Am. Chem. Soc.* **2003**, *125*, 8458. (c) Auria, R. D.; Turco, R. P. *J. Phys. Chem. A* **2004**, *108*, 3756. (d) Andrei, H. S.; Solca, N.; Dopfer, O. *Chem. Phys. Chem.* **2006**, *7*, 107. (e) Bianco, R.; Wang, S.; Hynes, J. T. *J. Phys. Chem. A* **2007**, *111*, 11033.
(42) (a) Rao, J. S.; Dinadayalane, T. C.; Leszczynski, J.; Sastry, G. N. *J. Phys. Chem. A* **2008**, *112*, 12944. (b) Pingale, S. S.; Gadre, S. R.; Bartolotti, L. J. *J. Phys. Chem. A* **1988**, *102*, 9987. (c) Sivanesan, D.; Babu, K.; Gadre, S. R.; Subramanian, V.; Ramasami, T. *J. Phys. Chem. A* **2000**, *104*, 10887. (d) Gadre, S. R.; Babu, K.; Rendell, A. P. *J. Phys. Chem. A* **2000**, *104*, 8976.
(43) (a) Zhao, Y.; Truhlar, D. G. *J. Phys. Chem. A* **2004**, *108*, 6908. (b) Zhao, Y.; Truhlar, D. G. *J. Chem. Theory Comput.* **2005**, *1*, 415. (c) Zhao, Y.; Truhlar, D. G. *Phys. Chem. Chem. Phys.* **2005**, *7*, 2701. (d) Zhao, Y.; Schultz, N. E.; Truhlar, D. G. *J. Chem. Theory Comput.* **2006**, *2*, 364. (e) Zhao, Y.; Truhlar, D. G. *J. Chem. Theory Comput.* **2007**, *3*, 289.
(44) (a) Zhao, Y.; Truhlar, D. G. *J. Phys. Chem. A* **2005**, *109*, 5656. (b) Zhao, Y.; Truhlar, D. G. *J. Chem. Theory Comput.* **2006**, *2*, 1009. (c) Zhao, Y.; Truhlar, D. G. *Theor. Chem. Acc.* **2008**, *120*, 215.
(45) Frisch, M. J.; Trucks, G. W.; Schlegel, H. B.; Scuseria, G. E.; Robb, M. A.; Cheeseman, J. R.; Zakrzewski, V. G.; Montgomery, J. A., Jr.; Stratmann, R. E.; Burant, J. C.; Dapprich, S.; Millam, J. M.; Daniels, A. D.; Kudin, K. N.; Strain, M. C.; Farkas, O.; Tomasi, J.; Barone, V.; Cossi, M.; Cammi, R.; Mennucci, B.; Pomelli, C.; Adamo, C.; Clifford, S.; Ochterski, J.; Petersson, G. A.; Ayala, P. Y.; Cui, Q.; Morokuma, K.; Malick, D. K.; Rabuck, A. D.; Raghavachari, K.; Foresman, J. B.; Cioslowski, J.; Ortiz, J. V.; Baboul, A. G.; Stefanov, B. B.; Liu, G.; Liashenko, A.; Piskorz, P.; Komaromi, I.; Gomperts, R.; Martin, R. L.; Fox, D. J.; Keith, T.; Al-Laham, M. A.; Peng, C. Y.; Nanayakkara, A.; Gonzalez, C.; Challacombe, M.; Gill, P. M. W.; Johnson, B.; Chen, W.; Wong, M. W.; Andres, J. L.; Head-Gordon, M.; Replogle, E. S.; Pople, J. A. *Gaussian 98*, revision A.7; Gaussian, Inc.: Pittsburgh, PA, 1998.
(46) Frisch, M. J.; Trucks, G. W.; Schlegel, H. B.; Scuseria, G. E.; Robb, M. A.; Cheeseman, J. R.; Montgomery, J. A., Jr.; Vreven, T.; Kudin, K. N.; Burant, J. C.; Millam, J. M.; Iyengar, S. S.; Tomasi, J.; Barone, V.; Mennucci, B.; Cossi, M.; Scalmani, G.; Rega, N.; Petersson, G. A.; Nakatsuji, H.; Hada, M.; Ehara, M.; Toyota, K.; Fukuda, R.; Hasegawa, J.; Ishida, M.; Nakajima, T.; Honda, Y.; Kitao, O.; Nakai, H.; Klene, M.; Li, X.; Knox, J. E.; Hratchian, H. P.; Cross, J. B.; Bakken, V.; Adamo, C.; Jaramillo, J.; Gomperts, R.; Stratmann, R. E.; Yazyev, O.; Austin, A. J.; Cammi, R.; Pomelli, C.; Ochterski, J. W.; Ayala, P. Y.; Morokuma, K.; Voth, G. A.; Salvador, P.; Dannenberg, J. J.; Zakrzewski, V. G.; Dapprich, S.; Daniels, A. D.; Strain, M. C.; Farkas, O.; Malick, D. K.; Rabuck, A. D.; Raghavachari, K.; Foresman, J. B.; Ortiz, J. V.; Cui, Q.; Baboul, A. G.; Clifford, S.; Cioslowski, J.; Stefanov, B. B.; Liu, G.; Liashenko, A.; Piskorz, P.; Komaromi, I.; Martin, R. L.; Fox, D. J.; Keith, T.; Al-Laham, M. A.; Peng, C. Y.; Nanayakkara, A.; Challacombe, M.; Gill, P. M. W.; Johnson, B.; Chen, W.; Wong, M. W.; Gonzalez, C.; Pople, J. A. *Gaussian 03*, revision E.01; Gaussian, Inc.: Wallingford, CT, 2004.
(47) (a) Lin, C.-K.; Wu, C.-C.; Wang, Y.-S.; Lee, Y. T.; Chang, H.-C.; Kuo, J.-L.; Klein, M. L. *Phys. Chem. Chem. Phys.* **2005**, *7*, 938. (b) Kuo, J. L.; Xie, Z. Z.; Bing, D.; Fujii, A.; Hamashima, T.; Suhara, K. I.; Mikami, N. *J. Phys. Chem. A* **2008**, *112*, 10125.
(48) (a) Jiang, J. C.; Wang, Y. S.; Chang, H. C.; Lin, S. H.; Lee, Y. T.; Niedner-Schatteburg, G.; Chang, H.-C. *J. Am. Chem. Soc.* **2000**, *122*, 1398. (b) Jiang, J. C.; Chaudhuri, C.; Lee, Y. T.; Chang, H.-C. *J. Phys. Chem. A* **2002**, *106*, 10937. (c) Wu, C. C.; Lin, C. K.; Chang, H.-C.; Jiang, J. C.; Kuo, J. L.; Klein, M. L. *J. Chem. Phys.* **2005**, *122*, 074315. (d) Chang, H.-C.; Wu, C.-C.; Kuo, J.-L. *Int. Rev. Phys. Chem.* **2005**, *24*, 553.
(49) Boys, S. F.; Bernardi, F. *Mol. Phys.* **1970**, *19*, 553.
(50) Dzidic, I.; Kebarle, P. *J. Phys. Chem.* **1970**, *74*, 1466.
(51) Parthasarathi, R.; Subramanian, V.; Sathyamurthy, N. *J. Phys. Chem. A* **2007**, *111*, 13287.
(52) Christie, R. A.; Jordan, K. D. *J. Phys. Chem. A* **2001**, *105*, 7551.

(53) Asmis, K. N.; Pivonka, N. L.; Santambrogio, G.; Brümmer, M.; Kaposta, C.; Neumark, D. M.; Wöste, L. *Science* **2003**, *299*, 1375.
(54) Fridgen, T. D.; McMahon, T. B.; MacAleese, L.; Lemaire, J.; Maitre, P. *J. Phys. Chem. A* **2004**, *108*, 9008.
(55) (a) Christie, R. A.; Jordan, K. D. *Intermolecular Forces* 2005, Ed. Wales, D. (b) Cui, J. Ph.D. Thesis, University of Pittsburgh, Pittsburgh, PA, 2007.
(56) Headrick, J. M.; Bopp, J. C.; Johnson, M. A. *J. Chem. Phys.* **2004**, *121*, 11523.
(57) Park, M.; Shin, I.; Singh, N. J.; Kim, K. S. *J. Phys. Chem. A* **2007**, *111*, 10692.
(58) (a) Jieli, M.; Aida, M. *J. Phys. Chem. A* **2009**, *113*, 1586. (b) Karthikeyan, S.; Kim, K. S. *J. Phys. Chem. A* **2009**, *113*, 9237.
(59) (a) Begemann, M. H.; Gudeman, C. S.; Pfaff, J.; Saykally, R. J. *Phys. Rev. Lett.* **1983**, *51*, 554. (b) Schwartz, H. A. *J. Chem. Phys.* **1977**, *67*, 1977.

JP904576U